the plant journal

SEB SOCIETY FOR EXPERIMENTAL BIOLOGY

The Plant Journal (2024) doi: 10.1111/tpj.16747

Yield-related quantitative trait loci identification and lint percentage hereditary dissection under salt stress in upland cotton

Anhui Guo[1], Huijing Li[1], Yi Huang[2], Xiaoqing Ma[1], Bin Li[1], Xiaoqi Du[1], Yanan Cui[1], Nan Zhao[1] and Jinping Hua[1,*]

[1]Laboratory of Cotton Genetics, Genomics and Breeding/Key Laboratory of Crop Heterosis and Utilization of Ministry of Education/Beijing Key Laboratory of Crop Genetic Improvement, College of Agronomy and Biotechnology, China Agricultural University, No. 2, Yuanmingyuan West Rd, Haidian District, Beijing 100193, China, and

[2]Oil Crops Research Institute, Chinese Academy of Agricultural Sciences, Wuhan 430062,Hubei, China

Received 18 September 2023; revised 7 January 2024; accepted 14 March 2024.

*For correspondence (e-mail jinping_hua@cau.edu.cn).

SUMMARY

Salinity is frequently mentioned as a major constraint in worldwide agricultural production. Lint percentage (LP) is a crucial yield-component in cotton lint production. While the genetic factors affect cotton yield in saline soils are still unclear. Here, we employed a recombinant inbred line population in upland cotton (*Gossypium hirsutum* L.) and investigated the effects of salt stress on five yield and yield component traits, including seed cotton yield per plant, lint yield per plant, boll number per plant, boll weight, and LP. Between three datasets of salt stress (E1), normal growth (E2), and the difference values dataset of salt stress and normal conditions (*D*-value), 87, 82, and 55 quantitative trait loci (QTL) were detectable, respectively. In total, five QTL (*qLY-Chr6-2*, *qBNP-Chr4-1*, *qBNP-Chr12-1*, *qBNP-Chr15-5*, *qLP-Chr19-2*) detected in both in E1 and *D*-value were salt related QTL, and three stable QTL (*qLP-Chr5-3*, *qLP-Chr13-1*, *qBW-Chr5-5*) were detected both in E1 and E2 across 3 years. Silencing of nine genes within a stable QTL (*qLP-Chr5-3*) highly expressed in fiber developmental stages increased LP and decreased fiber length (FL), indicating that multiple minor-effect genes clustered on Chromosome 5 regulate LP and FL. Additionally, the difference in LP caused by *Gh_A05G3226* is mainly in transcription level rather than in the sequence difference. Moreover, silencing of salt related gene (*GhDAAT*) within *qBNP-Chr4-1* decreased salt tolerance in cotton. Our findings shed light on the regulatory mechanisms underlining cotton salt tolerance and fiber initiation.

Keywords: upland cotton (*Gossypium hirsutum*), salt stress, quantitative trait loci, yield, lint percentage.

INTRODUCTION

Upland cotton (*Gossypium hirsutum* L.), one of the most important cash crops, accounts for more than 90% of the yield worldwide (Ma et al., 2021; Zhang et al., 2011). Salinity is one of the important abiotic stresses limiting the growth and development of cotton, and eventually reducing cotton yield and fiber quality (Ashraf et al., 2018; Guo, Hao, et al., 2022; Guo, Su, et al., 2022). More than 36 million ha (about 4.88% of the available land) are affected by salt stress in China (Li et al., 2014). Cotton is considered a pioneer crop in saline soils, which is tolerant to a salinity threshold level of 7.7 dS m^{-1} and supply the possibility to utilize the saline soils; however, salt stress will lead to a 50% yield reduction at 17.0 dS m^{-1} level (Khorsandi & Anagholi, 2009). Great efforts have been made on researches in salt tolerance of cotton, little progress has been achieved in developing salt-tolerant varieties. Therefore, uncovering the genetic basis of salt tolerance and improving yield potential in upland cotton are demonstrated an increasingly necessary.

Salt tolerance are complex quantitative traits that are controlled by multiple genes and are affected by environmental conditions, which are evaluated by using yield, fiber quality and some other important traits. Quantitative trait loci (QTL) mapping is an effective strategy for quantitative trait research and has been widely used in cotton (Ismail & Horie, 2017). Several studies on QTL mapping of cotton yield and yield component traits have been performed. It has been reported that 60 QTL were detected for the yield traits using a recombinant inbred line (RIL) population derived from a cross between the high-fiber-quality cv. Nongdamian 13 and the high fiber-yield cv. Nongda 601, of which 12 stable QTL were detected (Gu et al., 2020). And 364 QTL for yield and yield components using a RIL population derived from two upland cotton cultivars (0-153

and sGK9708), of which 211 controlled BW, and 153 controlled lint percentage (LP), respectively (Zhang et al., 2020). Two QTL with additive effects for LP were identified in a RIL population derived from the cross of NC05AZ21 × TX-2324 (Zhu et al., 2021). Moreover, a total of 28 QTL for LP were identified using a RIL population, which contains 137 lines derived from *G. hirsutum* cv. CCRI 36 and *G. hirsutum* acc. G2005. Furthermore, two genes (*Gh_A05G1584* and *Gh_A05G1689*), which are highly expressed during fiber development stages in the high LP variety (CCRI 36), were revealed as candidate genes for LP (Wang, Jia, et al., 2021). And numerous QTL related to salt tolerance at germination and seedling stages were identified in upland cotton (Diouf et al., 2017; Gu et al., 2021; Hussain et al., 2017; Oluoch et al., 2016). A total of eight clusters controlling salt-tolerance traits were distributed on chromosomes (Chr) A02, A06, A12, D03, D06, D08, and D13 were identified (Diouf et al., 2017). The salt tolerant QTL *qSalt-A04-1* has been detected on Chr A04 in seed germination stage (Gu et al., 2021). Moreover, 11 QTL were detected on eight chromosomes including Chr A09, A11, D02, D03, D08, D10, D11 and D13 (Oluoch et al., 2016). In our previous study, three salt-tolerant QTL and two clusters were detected using four germination traits and six seedling traits under both indoor and field salt stress conditions (Guo, Hao, et al., 2022; Guo, Su, et al., 2022). However, research was limited for yield-related traits by QTL mapping under salt stress conditions, even though it will improve yield and facilitate saline-alkali soil utilization.

Lint percentage is an important component of cotton lint yield and an index of constant breeding goal for the evaluation on lint yield improvement in cotton varieties. The yield potential is closely related to population productivity, finally is determinate by the formation of fiber cells. Fiber development consists of four stages: initiation, elongation, secondary cell wall (SCW) biosynthesis, and maturity of fiber, which contributed differentially to LP based on the development process of days post-anthesis (DPA) (Zou et al., 2022). The fiber initiation stage starts from 3 days before anthesis to 3 DPA with trichome protrusion and enlargement of epidermal cells. Fiber initiation has an important impact on the number of fiber cells to determine LP (Zhang et al., 2011). The IAA biosynthetic gene *iaaM*, expressed in the epidermis of cotton ovules at the fiber initiation stage in a tissue-specific manner, will increase the lint yield by more than 15% (Zhang et al., 2011). To data, an increasing number of transcription factors (TFs) have been reported to involve in fiber initiation, such as *GhWRKY16* (Wang, Li, et al., 2021) and *GhMYB5_A12* (Wang, Ma, et al., 2021). And functional genes have also been shown to be involved in fiber initiation. For example, *GhWAKL3* (cell wall-associated receptor-like kinase 3) was positively correlated with LP (Ma, Wang, Ijaz, & Hua, 2019; Ma, Wang, Li, et al., 2019).

To dissect the genetic mechanism of salt tolerance and to improve the yield under salt stress conditions, a RIL population (177 lines) derived from a cross between the high-yield cv. GX1135 and the low-yield cv. GX100-2 was used for evaluating five yield and yield-component traits under salt stress conditions and normal growth conditions across 3 years (Guo et al., 2021). QTL mapping was conducted using the same genetic linkage map consisting of 2859 bins (Guo et al., 2021). Then, we screen candidate genes within the stable QTL detected in chromosome A05 based on the expression patterns in different fiber development stages. Finally, four genes within *qLP-Chr5-3* were verified to play combined negative regulatory roles in the construction of LP using virus-induced gene silencing (VIGS) assay. The study provides elite loci for improving both yield and salt-tolerance in upland cotton, which is beneficial to the utilization of saline-alkali land.

RESULTS

Phenotype variation of the yield and yield-component traits

A RIL population developed between the two parents, GX1135 and GX100-2, was planted from 2016 to 2018 under salt stress conditions and normal growth conditions (Table 1). In most cases, the performances of female parent GX1135 were often superior to that of male parent GX100-2 for these six traits under both conditions (Table 1). In the RIL population, the skewness and kurtosis values for five yield and yield-component traits ranged from −1 to 1 in the RIL population on both conditions except for SY (1.17) and LY (1.12) under normal conditions, and BW (1.40) under salt stress condition in 2018 (Table 1). All traits exhibited varying abundance in the RIL population under salt and normal growth conditions, as observed in the difference values dataset of salt stress and normal conditions (*D*-value) and salt index (SI) datasets (Table 1; Tables S1 and S2).

The coefficients of variation (CV) of three yield-related traits (seed cotton yield per plant [SY], lint yield per plant [LY], boll number per plant [BNP], and plant productive forces [PPF]) under salt stress conditions were higher than those under normal growth conditions, indicating a more severe impact of salt on cotton yield. The CV for LP was the smallest, suggesting that it was less susceptible to salt stress. We compared the differences in six yield-related traits under salt stress and normal growth conditions and found that three traits (SY, LY, and BNP) decreased across 3 years' experiments under salt stress conditions, while the other two yield component traits (LP and BW) showed inconsistent performance during 3 years trials. To evaluate the effect of salt stress on cotton yield, the composite trait–PPF was used in the present research. We observed a significant impact of salt stress on PPF (Table 1). This result implied that the reduction in cotton yield is primarily

Table 1 Descriptive statistical analysis for the yield and yield-component traits under salt stress and normal growth conditions

			Populations							Parents		F_1	CK
Traits	Year	Environment	Mean	SD	CV%	Min.	Max.	Skewness	Kurtosis	GX1135	GX100-2	Xinza1	Ruiza 816
SY (g)	2016	E1	33.42	13.73	41.08	8.11	79.45	0.49	0.18	48.72	22.58	40.47	58.26
	2016	E2	40.95	14.76	36.06	9.39	91.59	0.44	0.61	41.29	32.40	43.00	58.48
	2017	E1	74.25	17.87	24.07	26.10	113.75	−0.18	−0.33	89.74	74.50	92.74	91.20
	2017	E2	76.28	17.68	23.18	21.41	114.39	−0.29	−0.21	69.14	79.01	104.78	90.29
	2018	E1	87.55	13.64	15.58	41.10	119.50	−0.26	0.48	105.16	116.91	90.32	113.85
	2018	E2	108.75	14.27	13.12	55.30	152.10	−0.30	1.17	143.45	126.38	132.01	122.98
LY (g)	2016	E1	13.27	5.80	43.69	1.59	31.76	0.43	−0.10	21.45	6.69	15.96	24.41
	2016	E2	16.29	6.35	39.00	3.42	38.63	0.58	0.98	16.28	11.67	17.26	22.43
	2017	E1	31.17	8.40	26.95	8.75	53.24	−0.06	−0.19	39.29	33.13	40.89	40.67
	2017	E2	31.97	7.90	24.72	8.77	49.68	−0.16	−0.12	30.54	29.34	46.80	39.56
	2018	E1	36.06	5.89	16.34	14.70	49.30	−0.35	0.36	45.81	43.77	38.30	45.73
	2018	E2	45.67	6.42	14.07	21.20	62.30	−0.50	1.12	63.40	47.65	58.40	51.12
BNP	2016	E1	7.85	3.14	40.05	2.56	18.31	0.62	0.21	10.50	4.88	8.53	10.75
	2016	E2	10.46	3.53	33.79	2.63	21.56	0.20	0.19	10.47	8.28	9.25	11.69
	2017	E1	19.19	3.48	18.14	7.00	27.18	−0.34	0.03	23.15	20.33	19.00	17.29
	2017	E2	20.02	3.24	16.20	9.55	29.88	0.05	0.04	22.29	20.31	20.42	17.17
	2018	E1	22.67	2.58	11.39	14.00	30.63	−0.26	0.42	25.88	26.74	22.31	22.69
	2018	E2	27.39	3.31	12.09	16.50	35.56	−0.19	0.40	33.38	29.75	29.75	24.94
BW (g)	2016	E1	4.61	0.54	11.78	3.19	6.36	0.13	0.31	4.59	4.98	5.20	5.72
	2016	E2	4.36	0.54	12.39	3.28	5.85	0.16	−0.42	4.87	4.67	4.81	5.60
	2017	E1	4.94	0.58	11.65	3.15	6.43	−0.31	0.28	5.27	4.84	5.62	6.45
	2017	E2	5.14	0.55	10.78	3.45	6.42	−0.22	−0.06	5.12	6.58	5.87	6.36
	2018	E1	4.54	0.48	10.48	2.81	6.34	0.14	1.40	4.87	5.19	5.16	5.25
	2018	E2	4.68	0.51	10.88	3.44	6.11	0.18	−0.22	4.98	5.16	5.57	5.65
LP (%)	2016	E1	39.24	2.74	6.97	32.88	45.75	0.04	−0.45	39.91	35.88	39.30	39.12
	2016	E2	39.43	2.78	7.06	31.78	47.02	0.30	−0.06	39.03	35.96	40.00	38.57
	2017	E1	41.91	2.97	7.08	33.50	48.72	−0.02	−0.31	43.74	44.69	44.09	44.64
	2017	E2	41.82	2.81	6.73	35.05	51.01	0.17	−0.26	44.21	37.14	44.68	43.82
	2018	E1	41.20	2.20	5.35	35.60	48.38	0.28	0.13	43.78	37.44	42.40	40.11
	2018	E2	41.97	2.37	5.65	36.65	47.47	−0.02	−0.51	44.15	37.70	44.29	41.50
PPF (g)	2016	E1	36.36	15.55	42.77	9.77	86.03	0.68	0.23	48.22	24.62	45.74	60.97
	2016	E2	45.96	17.28	37.59	9.93	95.61	0.36	−0.02	53.14	38.35	44.51	65.62
	2017	E1	94.88	20.30	21.39	34.00	143.97	−0.19	0.02	122.09	98.36	106.86	111.42
	2017	E2	102.97	19.10	18.55	34.94	145.89	−0.36	0.06	114.04	133.62	119.93	109.15
	2018	E1	103.00	15.96	15.50	48.72	145.78	−0.20	0.68	126.06	138.84	115.18	119.11
	2018	E2	127.99	19.09	14.91	67.20	185.38	−0.01	0.95	166.27	153.57	165.71	140.95

BNP, boll number per plant; BW, boll weight; CV, coefficient of variation; E1, salt stress conditions; E2, normal growth conditions; LP, lint percentage; LY, lint yield per plant; PPF, cotton plant productive forces; SD, mean values ± standard deviation values; SY, seed cotton yield per plant.

attributed to a decrease in boll number under salt stress conditions. The ANOVA results revealed that all the traits presented significant environmental and genetic effects (Table 2). The variance due to the interaction of genotype (G) and year (Y), E × Y, was significant for all five traits, while the variance due to G × E × Y was not significant for only one trait (LP). Broad-sense heritability ranged from 40.19 (BNP) to 81.32 (LP), suggesting that genotype predominantly influences yield-related traits.

Correlations across yield traits

Table 3 displays the correlation analysis of yield and yield-component traits based on the datasets of mean phenotypic values under E1 and E2, as well as the *D*-value dataset. The correlations between salt-stress yield and normal-stress yield were consistently positive, ranging from 0.259 (BNP in 2017) to 0.864 (LP in 2018) (Table S3). Notably, the correlation between PPF and SY (0.733–0.962) was the highest, providing evidence that PPF serves as a reliable indicator for effective yield in cotton. We observed a high correlation (*R* values ranging from 0.682 to 0.970) between the values of SY, LY, and BNP under both salt stress and normal conditions. This result suggested that salt stress did not affect the correlation among these three traits and was in line with the finding that the seed yield and lint yield of cotton are mainly affected by a decrease in boll number. SY showed significant positive correlations with LY, BNP, and BW, except for BW in *D*-value dataset in 2016. Regarding LY, positive correlations were observed with BNP, BW, and LP, with no correlation observed with

Table 2 Analysis of variance and broad-sense heritability h_b^2 for the yield and yield component traits in the RIL population

Trait	Source	df	Sum sq.	Mean sq.	*F*-value	*P*(>*F*)	h_b^2
SY	G	176	239449.00	1361.00	5.33	***	57.31
	E	1	139452.00	139452.00	546.02	***	
	Y	2	1227845.00	613923.00	2403.80	***	
	G × E	176	41652.00	237.00	0.93		
	G × Y	352	143141.00	407.00	1.59	***	
	E × Y	2	10537.00	5269.00	20.63	***	
	G × E × Y	352	76332.00	217.00	0.85		
	Error	1	662.00	662.00	2.59		
LY	G	176	45852.00	261.00	5.36	***	58.08
	E	1	18915.00	18915.00	389.13	***	
	Y	2	213341.00	106670.00	2194.50	***	
	G × E	176	8033.00	46.00	0.94		
	G × Y	352	26054.00	74.00	1.52	***	
	E × Y	2	2279.00	1139.00	23.44	***	
	G × E × Y	348	13194.00	38.00	0.78		
	Error	1	168.00	168.00	3.46		
BNP	G	176	8321.00	47.00	3.15	***	40.19
	E	1	10074.00	10074.00	671.93	***	
	Y	2	84140.00	42070.00	2806.16	***	
	G × E	176	2175.00	12.00	0.82		
	G × Y	352	6766.00	19.00	1.28	**	
	E × Y	2	472.00	236.00	15.73	***	
	G × E × Y	352	4595.00	13.00	0.87		
	Error	1	93.00	93.00	6.20	*	
BW	G	176	326.30	1.85	8.36	***	60.91
	E	1	1.00	1.00	4.49	*	
	Y	2	117.20	58.59	264.04	***	
	G × E	176	46.30	0.26	1.18		
	G × Y	352	121.70	0.35	1.56	***	
	E × Y	2	17.20	8.59	38.73	***	
	G × E × Y	352	79.30	0.23	1.02		
	Error	1	0.70	0.68	3.04		
LP	G	176	10535.00	59.90	21.78	***	81.32
	E	1	56.00	55.80	20.31	***	
	Y	2	2465.00	1232.40	448.44	***	
	G × E	176	510.00	2.90	1.05		
	G × Y	352	2117.00	6.00	2.19	***	
	E × Y	2	32.00	16.20	5.88	**	
	G × E × Y	350	1152.00	3.30	1.20	*	
	Error	1	0.00	0.20	0.07		

BNP, boll number per plant; BW, boll weight; E, environment; G, genotype; h_b^2, broad-sense heritability; LP, lint percentage; LY, lint yield per plant; SY, seed cotton yield per plant; Y, year.
*, ** and *** Statistically significant at $P = 0.05$, 0.01, 0.001, respectively.

BW in the *D*-value dataset in 2016 and 2017. BNP showed a significantly positive correlation with LP, while there was no correlation with BW in both conditions. LP was correlated significantly and negatively with BW under E1, while negatively with BW, except in 2017. No correlations were observed between LP and BW in the *D*-value dataset. Our results demonstrated that salt stress heightened the negative correlation between LP and BW.

Single locus QTL distribution and effects on yield traits

A total of 180 QTL resolved with logarithm of odds (LOD) 2.0 for yield and yield-component traits were detected in three datasets, which explained 2.71–16.03% of total phenotypic variance (PV, hereinafter same) (Figure S1; Table S4; Table 4). Separating, 86, 82, and 56 QTL were detected under E1, E2, and in *D*-value dataset, respectively. A total of 87 QTL were distributed in the At sub-genome, and 93 were distributed in the Dt sub-genome. Taken together, 29 QTL were detected across at least 2 years, with 6, 4, 5, 4, 6, and 4 controlled SY, LY, BW, BNP, LP, and PPF, respectively. In total, 28 QTL were identified in at least two datasets. Among them, 19 QTL were detected in E1 and E2, five QTL were detected on E1 and *D*-value, and four were detected on E2 and *D*-value. Three of them were stable QTL. Only two QTL (*qSY-Chr16-1*, *qPPF-Chr16-2*), explaining the PV of 4.82–5.71% and 6.83–9.52%, were

Table 3 Correlation analysis among yield and yield-component traits under salt stress conditions, normal growth conditions, and by phenotypic differences between two conditions

Environment	Year	Trait	SY 2017	SY 2018	SY 2016	LY 2017	LY 2018	LY 2016	BNP 2017	BNP 2018	BNP 2016	BW 2017	BW 2018	BW 2016	LP 2017	LP 2018	LP 2016	PPF 2017	PPF 2018
E1	2017	SY	0.309**																
	2018	SY	0.316**	0.562**															
	2016	LY	0.435**	0.087	0.085														
	2017	LY	0.186*	0.577**	0.413**	0.057													
	2018	LY	0.310**	0.566**	0.950**	0.119	0.440**												
	2016	BNP	0.959**	0.255**	0.242**	0.446**	0.132	0.262**											
	2017	BNP	0.183*	0.816**	0.376**	0.051	0.501**	0.451**	0.194**										
	2018	BNP	0.236**	0.306**	0.682**	0.040	0.200**	0.744**	0.261**	0.438**									
	2016	BW	0.244**	0.195**	0.254**	0.091	0.179*	0.181*	0.109	0.000	−0.035								
	2017	BW	0.194**	0.409**	0.460**	0.095	0.308**	0.355**	0.053	0.010	−0.108	0.519**							
	2018	BW	0.210**	0.490**	0.655**	0.087	0.365**	0.556**	0.102	0.204**	0.047	0.343**	0.640**						
	2016	LP	0.119	0.006	−0.028	0.561**	0.018	0.025	0.142	0.036	0.001	0.052	−0.030	−0.001					
	2017	LP	0.003	0.000	0.108	0.007	0.805**	0.145	−0.013	0.059	0.067	0.053	0.033	0.070	0.020				
	2018	LP	0.064	0.103	0.020	0.121	0.137	0.324**	0.135	0.315**	0.333**	−0.198**	−0.275**	−0.212**	0.161*	0.127			
	2016	PPF	0.962**	0.298**	0.299**	0.432**	0.189*	0.299**	0.961**	0.189*	0.238**	0.356**	0.184*	0.185*	0.127	0.019	0.075		
	2017	PPF	0.255**	0.905**	0.553**	0.100	0.588**	0.558**	0.189*	0.842**	0.301**	0.268**	0.539**	0.505**	0.014	0.074	0.112	0.253**	
	2018	PPF	0.316**	0.540**	0.923**	0.089	0.386**	0.901**	0.261**	0.442**	0.746**	0.205**	0.343**	0.696**	0.001	0.097	0.092	0.300**	0.545**
E2	2017	SY	0.337**																
	2018	SY	0.212**	0.368**															
	2016	LY	0.947**	0.315**	0.191*														
	2017	LY	0.365**	0.962**	0.341**	0.370**													
	2018	LY	0.223**	0.340**	0.920**	0.257**	0.394**												
	2016	BNP	0.940**	0.292**	0.177*	0.924**	0.339**	0.226**											
	2017	BNP	0.157*	0.674**	0.147	0.189*	0.680**	0.160*	0.191*										
	2018	BNP	0.079	0.038	0.622**	0.147	0.096	0.695**	0.152*	0.173*									
	2016	BW	0.369**	0.184*	0.255**	0.224**	0.134	0.144	0.167*	−0.117	−0.061								
	2017	BW	0.078	0.372**	0.323**	0.006	0.313**	0.229**	−0.038	−0.022	−0.202**	0.355**							
	2018	BW	0.238**	0.419**	0.557**	0.188*	0.354**	0.433**	0.122	0.036	−0.143	0.401**	0.551**						
	2016	LP	0.022	−0.069	−0.041	0.236**	0.095	0.218**	0.178*	0.118	0.296**	−0.411**	−0.284**	−0.241**					
	2017	LP	0.187*	0.117	0.030	0.276**	0.373**	0.315**	0.260**	0.187*	0.269**	−0.137	−0.113	−0.132	0.579**				
	2018	LP	0.075	0.005	0.016	0.207**	0.200**	0.402**	0.171*	0.058	0.318**	−0.234**	−0.177*	−0.195**	0.653**	0.729**			
	2016	PPF	0.956**	0.319**	0.226**	0.887**	0.346**	0.235**	0.932**	0.133	0.105	0.494**	0.071	0.229**	0.020	0.189*	0.074		
	2017	PPF	0.174*	0.778**	0.292**	0.163*	0.748**	0.256**	0.138	0.829**	0.031	0.089	0.533**	0.321**	−0.054	0.090	−0.037	0.147	
	2018	PPF	0.211**	0.326**	0.904**	0.235**	0.323**	0.868**	0.185*	0.166*	0.694**	0.232**	0.232**	0.607**	0.064	0.107	0.102	0.224**	0.258**
D-value	2017	SY	0.037																
	2018	SY	0.096	0.036															
	2016	LY	0.440**	0.004	0.084														
	2017	LY	0.060	0.693**	0.112	0.008													
	2018	LY	0.101	0.047	0.970**	0.099	0.115												
	2016	BNP	0.958**	0.018	0.066	0.420**	0.038	0.071											
	2017	BNP	0.003	0.791**	−0.025	−0.041	0.557**	−0.035	−0.026										
	2018	BNP	0.085	0.038	0.825**	0.072	0.085	0.820**	0.040	−0.028									
	2016	BW	0.175*	−0.075	0.109	0.066	0.140	0.103	0.110	−0.063	0.146								

(continued)

Table 3. (continued)

Environment	Year	Trait	SY 2017	SY 2018	SY 2016	LY 2017	LY 2018	LY 2016	BNP 2017	BNP 2018	BNP 2016	BW 2017	BW 2018	BW 2016	LP 2017	LP 2018	LP 2016	PPF 2017	PPF 2018
	2017	BW	−0.048	0.016	0.075	0.039	0.065	0.100	−0.003	−0.002	0.057	0.158*							
	2018	BW	0.017	0.082	0.239**	−0.002	0.087	0.231**	0.027	0.092	−0.124	0.033	0.007						
	2016	LP	−0.019	0.072	0.015	0.527**	0.043	0.032	−0.016	0.019	0.032	−0.023	0.056	−0.035					
	2017	LP	0.042	0.052	0.100	−0.001	0.735**	0.085	0.035	0.052	0.063	0.228**	0.065	0.053	−0.020				
	2018	LP	0.017	0.106	0.147	0.081	0.046	0.356**	−0.008	0.068	0.205**	−0.037	0.088	0.022	0.061	−0.075			
	2016	PPF	0.930**	0.000	0.084	0.407**	0.112	0.085	0.933**	−0.037	0.076	0.421**	0.020	0.029	−0.022	0.143	−0.024		
	2017	PPF	−0.008	0.733**	0.011	−0.013	0.538**	0.012	−0.014	0.902**	0.001	0.006	0.419**	0.088	0.038	0.077	0.092	−0.020	
	2018	PPF	0.078	0.056	0.863**	0.046	0.102	0.847**	0.042	0.005	0.751**	0.144	0.026	0.538**	−0.006	0.076	0.161*	0.077	0.020

BNP, boll number per plant; BW, boll weight; CV, coefficient of variation; D, difference dataset between salt stress conditions and normal growth conditions; E1, salt stress conditions; E2, normal growth conditions; LP, lint percentage; LY, lint yield per plant; PPF, cotton plant productive forces; SY, seed cotton yield per plant.
**, * Respect a statistically significant correlation at the 0.01 and 0.05 levels, respectively (bilateral); critical value for correlation coefficients at probabilities of 0.05 and 0.01 are 0.145 and 0.190, respectively.

detected in all three datasets, which controlled the yield traits and salt tolerance simultaneously.

The QTL detected in both E1 and *D*-value were defined as salt-related QTL. We identified five salt-related QTL (*qLY-Chr6-2*, *qBNP-Chr4-1*, *qBNP-Chr12-1*, *qBNP-Chr15-5*, *qLP-Chr19-2*), which explained the PV ranging from 3.34 to 9.82% (Figure 1; Table 4). QTL detected in E1 and E2 across 2 years was defined as yield-related QTL. In total, two QTL controlled LP (*qLP-Chr5-3*, *qLP-Chr13-1*) and one controlled BW (*qBW-Chr5-5*) were detected as stable QTL. Of which, two QTL (*qLP-Chr5-3* and *qBW-Chr5-5*) were detected under E1 and E2 across 3 years and can be used for high-yield molecular breeding of cotton (Figure 1; Table 4).

In addition, another dataset of salt indices was established to detect salt-related QTL. A total of 43 QTL were detected in the SI dataset for yield and yield components, among which 11, 9, 2, 7, and 4 controlled SY, LY, BNP, BW, and LP, respectively, and the explained phenotypic variation ranged from 3.67 to 11.81% (Table S5). There were two major QTL (*qSIBNP-Chr5-1* and *qSIBNP-Chr21-3*), both of which controlled BNP traits and accounted for 10.35% and 11.81% of phenotypic variation, respectively. A total of 25 QTL were detected in both the *D*-value and SI datasets, of which 6, 5, 9, 2, and 3 were for SY, LY, BNP, BW, and LP. Two hotspot regions were detected in Chr5 and Chr21, of which four (*qSIBNP-Chr5-1*, *qSIBW-Chr5-1*, *qSILY-Chr5-1*, *qSISY-Chr5-1*) QTL were detected in the hotspot located on Chr5 and three (*qSIBNP-Chr21-1*, *qSIBNP-Chr21-2*, *qSIBNP-Chr21-3*) were included in the other hotspot on Chr21, respectively. Additionally, five QTL were detected under both SI and salt stress conditions, two QTL were detected in SI, salt stress, and normal growth conditions, and 11 QTL were newly detected in the SI dataset. In general, the number of BNP controlled in salt stress-related QTL was the highest, which also indicated that BNP was closely related to salt stress.

Pleiotropic effects upon yield traits

Among the QTL identified for six yield and yield-component traits, there were QTL for different traits that shared the confidence intervals at 95% level and were considered QTL clusters (Zhang et al., 2020). Totally, 40 clusters distributed on 24 chromosomes showed pleiotropic effects, involving a total of 136 QTL (Table 5). Among these, 19 and 21 QTL clusters were detected located on At and Dt sub-genome, respectively. Specifically, three clusters were identified in Chr4, Chr5, and Chr21. Additionally, two clusters were detected in 10 chromosomes (Chr1, Chr6, Chr10, Chr14, Chr15, Chr16, Chr19, Chr23, Chr24, and Chr25), while one cluster was detected in each of the other 11 chromosomes. Four clusters (Cluster-Chr5-3, Cluster-Chr16-1, Cluster-Chr24-1, Cluster-Chr26-1), eight clusters (Cluster-Chr1-1, Cluster-Chr5-2, Cluster-Chr11-1, Cluster-Chr12-1, Cluster-Chr14-1, Cluster-Chr23-1, Cluster-Chr23-2,

and Cluster-Chr25-2), and seven clusters (Cluster-Chr4-1, Cluster-Chr4-2, Cluster-Chr15-2, Cluster-Chr16-2, Cluster-Chr19-2, Cluster-Chr20-1, and Cluster-Chr22-1) improved five, four and three yield and yield-component traits, respectively (Table 5). The remaining 21 clusters controlled two yield and yield-component traits simultaneously.

A total of 14 clusters harbored QTL for SY and LY. QTL for SY and LY within eight clusters (Cluster-Chr1-1, Cluster-Chr11-1, Cluster-Chr16-2, Cluster-Chr19-2, Cluster-Chr23-1, Cluster-Chr23-2, Cluster-Chr24-1, Cluster-Chr26-1) were contributed by the female parent GX1135, while the QTL within four clusters (Cluster-Chr2-1, Cluster-Chr5-2, Cluster-Chr5-3, Cluster-Chr6-2) were contributed by the male parent GX100-2 under E1 or E2. The GX1135 allele increased LY but decreased SY in Cluster-Chr5-2, in which one QTL (*qLY-Chr5-1*) for LY was detected in *D*-value, one (*qSY-Chr5-1*) for SY was detected in both E2 and *D*-value, one for BNP (*qBNP-Chr5-3*) was detected in *D*-value, and one for BW (*qBW-Chr5-1*) was detected in E1.

Among the 14 clusters containing QTL for SY and LY, seven were identified based on the constituent traits (QTL detected under E1 or E2). Among the seven QTL clusters, three clusters (Cluster-Chr5-3, Cluster-Chr11-1, and Cluster-Chr24-1) contain stable QTL controlling SY or LY, which could be valuable for molecular breeding to simultaneously improve both SY and LY. The QTL cluster (Cluster-Chr24-1) hosted stable QTL both for SY and LY, including two QTL for SY (*qSY-Chr24-1*, *qSY-Chr24-2*), two for LY (*qLY-Chr24-1*, *qLY-Chr24-2*), two for BNP (*qBNP-Chr24-1*) and one for BW (*qBW-Chr24-1*). And the additive effects indicated that GX1135 alleles increased these four traits under salt stress and normal environments. The QTL cluster (Cluster-Chr11-1) had one stable QTL for LY (*qLY-Chr11-1*), one for SY (*qSY-Chr11-1*), and one for LP (*qLP-Chr11-1*), respectively, with the favorable alleles for SY, LY, and LP derived from GX1135. The QTL cluster Cluster-Chr5-3 contained the largest number of QTL (13) accounting for the PV of 4.15–32.74%, in which three (*qLP--Chr5-2*, *qLP-Chr5-3*, *qLP-Chr5-4*) controlled LP showed positive additive effects, three (*qSY-Chr5-2*, *qSY-Chr5-3*, *qSY-Chr5-4*), one (*qLY-Chr5-2*), and six QTL (*qBW-Chr5-4*, *qBW-Chr5-5*, *qBW-Chr5-6*, *qBW-Chr5-7*, *qPPF-Chr5-1*, *qPPF-Chr5-2*) controlled SY, LY, and BW had negative additive effects, respectively.

Table 4 Salt-related QTL and sable QTL for yield and yield-component traits under salt stress conditions, normal growth conditions

			Flanking markers		Under E1			Under E2			Mapping by the *D*-value		
Category	QTL	Year	L	R	LOD	Effect value	Var%	LOD	Effect value	Var%	LOD	Effect value	Var %
Salt related QTL	*qLY-Chr6-2*	2018	bin725	bin726							4.13	−2.13	9.11
		2018	bin728	bin729	2.80	−1.48	5.73						
	*qBNP-Chr4-1**	2017	bin381	bin382	3.51	0.86	6.82						
		2016	bin384	bin385							4.63	−1.11	9.30
	qBNP-Chr12-1	2016	bin1297	bin1298	2.32	0.70	4.76				3.15	0.91	6.19
	qBNP-Chr15-5	2017	bin1690	bin1691	2.32	−0.79	4.70				3.22	−1.09	6.57
	qLP-Chr19-2	2018	bin2112	bin2113							4.76	0.39	9.82
		2018	bin2113	bin2114	2.56	0.41	3.34						
Stable QTL	***qBW-Chr5-5****	2016	bin633	bin634	4.86	−0.18	10.26						
		2016	bin638	bin639				5.82	−0.18	10.49			
		2017	bin636	bin637	5.12	−0.18	7.74	7.49	−0.22	14.33			
		2018	bin636	bin637	4.18	−0.14	8.20						
	qLP-Chr5-3*	2016	bin633	bin634	7.10	1.03	13.30						
		2016	bin635	bin636				9.45	1.10	15.37			
		2016	bin640	bin641	9.42	1.11	15.84						
		2017	bin633	bin634	16.20	1.63	29.91						
		2017	bin635	bin636				12.30	1.32	21.19			
		2018	bin635	bin636	19.90	1.28	32.74						
		2018	bin640	bin641				16.33	1.26	27.18			
	qLP-Chr13-1*	2017	bin1378	bin1379				4.67	0.78	7.52			
		2017	bin1389	bin1390	5.81	0.92	9.40						
		2018	bin1381	bin1382	4.71	0.56	6.39						
		2018	bin1382	bin1383				5.36	0.66	7.66			

The figures underlined referred to the common QTL detected on two datasets in the same year in the present study. QTL with bold font represent Var% of QTL was more than 10. QTL noted by "*" referred to common QTL detected at least 2 years; and Var%, phenotypic variation explained by a single locus QTL.

BNP, boll number per plant; BW, boll weight; E1, salt stress conditions; E2, normal growth conditions; LP, lint percentage; LY, lint yield per plant; PPF, cotton plant productive forces; QTL, quantitative trait loci.

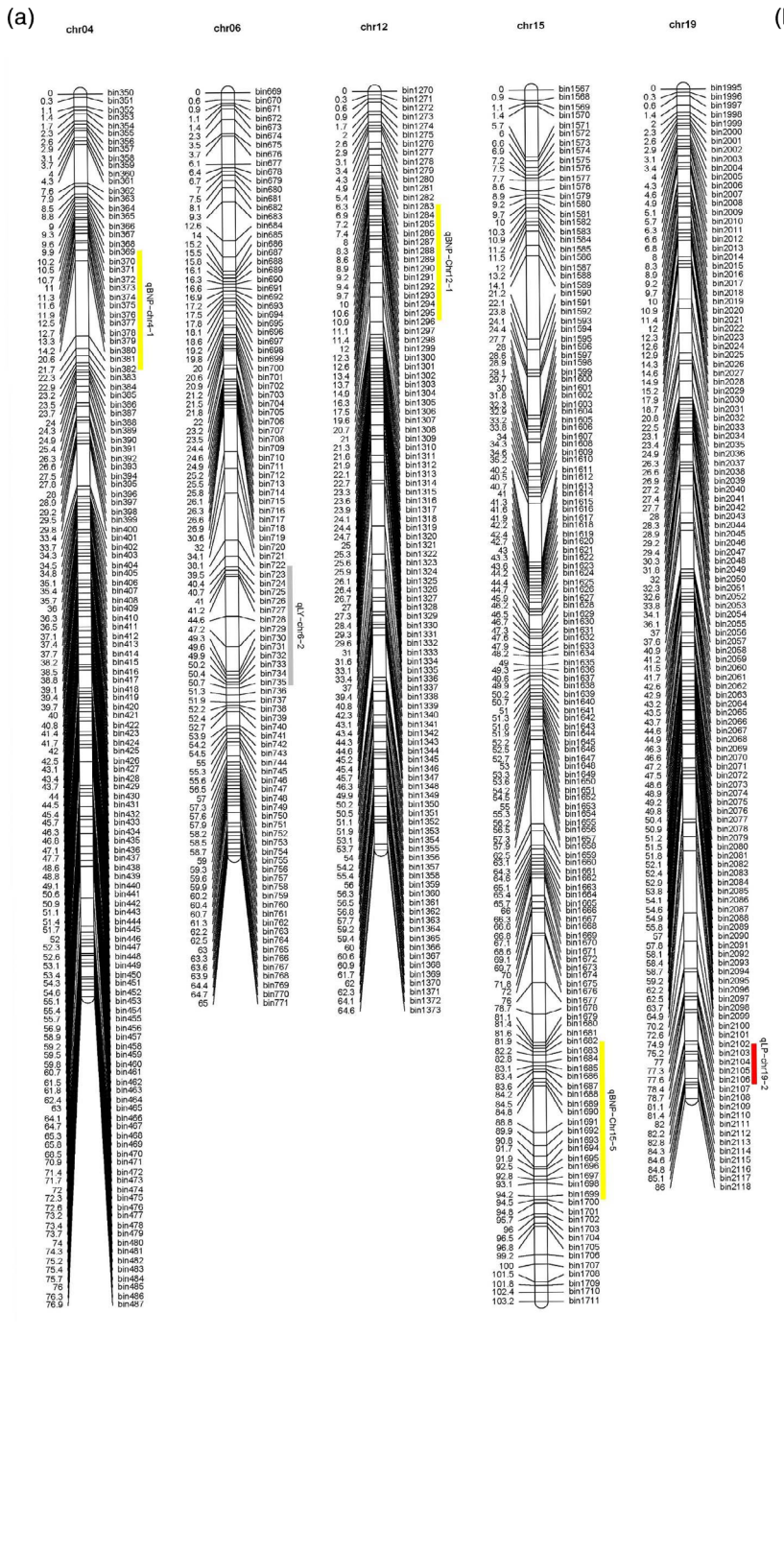

Figure 1. The position of salt-related QTL and stable QTL on the linkage groups.
The location of salt-related QTL (a) and stable QTL (b) on the linkage groups. BNP, boll number per plant; BW, boll weight; LP, lint percentage; LY, lint yield per plant; QTL, quantitative trait loci.

Table 5 Pleiotropic regions for the yield and yield-component traits

			Flanking Marker		Under E1			Under E2			Mapping by the *D*-value		
Cluster	QTL	Year	L	R	LOD	Effect value	Var%	LOD	Effect value	Var%	LOD	Effect value	Var %
Cluster-Chr1-1	*qSY-Chr1-1**	2016	bin53	bin54				3.95	4.01	8.05			
		2017	bin58	bin59							2.78	4.09	5.76
		2018	bin65	bin66	2.68	3.57	5.55						
	qLP-Chr1-2	2018	bin58	bin59				2.88	0.43	3.81			
	qLY-Chr1-1	2017	bin58	bin59							3.70	2.08	7.54
	qBNP-Chr1-1	2016	bin59	bin60				6.76	1.53	13.67			
Cluster-Chr1-2	*qBNP-Chr1-3*	2017	bin96	bin97	2.52	−0.73	4.84						
	qLP-Chr1-3	2016	bin101	bin102							2.74	0.51	5.82
Cluster-Chr2-1	*qLY-Chr2-2*	2016	bin135	bin136	4.38	−1.93	8.71						
	qSY-Chr2-1	2016	bin144	bin145	2.25	−3.15	4.24						
Cluster-Chr4-1	*qLY-Chr4-1*	2016	bin382	bin383	2.36	1.37	4.59						
		2016	bin382	bin383							4.54	−2.06	9.17
	qPPF-Chr4-1	2016	bin384	bin385							2.13	−3.82	4.23
		2016	bin381	bin382							2.83	−4.20	6.24
	*qBNP-Chr4-1**	2017	bin381	bin382	3.51	0.86	6.82						
		2016	bin384	bin385							4.63	−1.11	9.30
Cluster-Chr4-2	*qPPF-Chr4-2*	2016	bin398	bin399							2.07	−3.65	4.53
	*qBNP-Chr4-2**	2016	bin396	bin397							4.58	−1.11	9.22
		2017	bin400	bin401	2.22	0.70	4.38						
	qBNP-Chr4-3	2016	bin403	bin404							2.60	−0.85	5.37
	qSY-Chr4-1	2016	bin396	bin397							3.67	−4.28	7.49
Cluster-Chr4-3	*qSY-Chr4-2*	2018	bin482	bin483	2.40	3.20	4.83						
	*qLP-Chr4-1**	2016	bin484	bin485	2.54	−0.55	3.77						
		2018	bin484	bin485	3.14	−0.51	4.43						
Cluster-Chr5-1	*qBNP-Chr5-1*	2018	bin489	bin490	3.60	0.93	7.66						
	qLP-Chr5-1	2016	bin495	bin496				4.78	0.77	7.66			
		2016	bin498	bin499	2.62	0.55	3.89						
	qBNP-Chr5-2	2018	bin498	bin499	2.60	0.82	6.00						
Cluster-Chr5-2	*qBW-Chr5-1*	2017	bin518	bin519				2.01	−0.10	2.78			
	qSY-Chr5-1	2017	bin518	bin519							2.80	4.21	6.15
		2017	bin518	bin519	2.18	−3.48	3.73						
	qLY-Chr5-1	2017	bin518	bin519							3.92	2.21	8.55
	qBNP-Chr5-3	2017	bin518	bin519							4.77	1.29	9.45
Cluster-Chr5-3	*qSY-Chr5-2*	2018	bin631	bin631				3.02	−3.38	5.84			
	qLP-Chr5-2	2017	bin629	bin630	6.83	1.02	12.59						
		2017	bin629	bin630				8.74	1.22	16.30			
	qLP-Chr5-3*	2016	bin633	bin634				7.10	1.03	13.30			
		2017	bin633	bin634				16.20	1.63	29.91			
		2017	bin635	bin636	12.30	1.32	21.19						
		2016	bin635	bin636	9.45	1.10	15.37						
		2018	bin635	bin636				19.90	1.28	32.74			
		2018	bin640	bin641	16.33	1.26	27.18						
		2016	bin640	bin641				9.42	1.11	15.84			
	qBW-Chr5-4	2017	bin629	bin630				3.28	−0.15	5.08			
	qBW-Chr5-5*	2016	bin633	bin634				4.86	−0.18	10.26			
		2017	bin636	bin637	7.49	−0.22	14.33						
		2018	bin636	bin637				4.18	−0.14	8.20			
		2017	bin636	bin637				5.12	−0.18	7.74			
		2016	bin638	bin639	5.82	−0.18	10.49						
	qBW-Chr5-6*	2016	bin645	bin646				6.03	−0.19	11.82			
		2018	bin644	bin645	4.09	−0.15	8.47						
		2017	bin646	bin647				9.77	−0.26	19.56			
	qLY-Chr5-2	2016	bin644	bin645				2.26	−1.27	4.72			
		2016	bin663	bin664				2.86	−1.40	5.67			

(continued)

Table 5. (continued)

Cluster	QTL	Year	Flanking Marker		Under E1			Under E2			Mapping by the *D*-value		
			L	R	LOD	Effect value	Var%	LOD	Effect value	Var%	LOD	Effect value	Var %
	qLP-Chr5-4*	2016	bin648	bin649	8.10	1.04	13.40						
		2018	bin648	bin649	8.92	0.97	16.26						
	qSY-Chr5-3	2018	bin635	bin636				2.18	−2.84	4.26			
	*qSY-Chr5-4**	2017	bin655	bin656	2.42	−3.69	4.15						
		2017	bin665	bin666				3.27	−4.43	5.83			
		2018	bin666	bin667				2.39	−3.11	4.45			
	*qBW-Chr5-7**	2018	bin664	bin665	4.90	−0.16	9.28						
		2016	bin663	bin664				3.85	−0.15	7.77			
		2017	bin667	bin668				6.39	−0.21	9.85			
	qPPF-Chr5-1	2017	bin646	bin647				2.35	−4.47	4.44			
	qPPF-Chr5-2	2017	bin665	bin666				5.55	−6.71	10.08			
Cluster-Chr6-1	*qLY-Chr6-1*	2018	bin716	bin717							2.40	1.41	4.98
	qBW-Chr6-2	2017	bin716	bin717				3.67	0.14	5.54			
Cluster-Chr6-2	*qLY-Chr6-2*	2018	bin725	bin726							4.13	−2.13	9.11
		2018	bin728	bin729				2.80	−1.48	5.73			
	qSY-Chr6-1	2018	bin725	bin726							2.63	−3.78	5.82
Cluster-Chr7-1	*qPPF-Chr7-2*	2018	bin832	bin833				2.23	−3.34	4.24			
	qBNP-Chr7-1	2018	bin834	bin835				2.66	−0.61	5.34			
Cluster-Chr8-1	*qBW-Chr8-2*	2017	bin969	bin970				3.23	−0.13	4.78			
	qLY-Chr8-1	2018	bin974	bin975							2.38	−1.21	4.91
Cluster-Chr9-1	*qSY-Chr9-1*	2016	bin990	bin991							2.20	−3.29	4.38
	qLY-Chr9-1	2016	bin990	bin991							2.13	−1.38	4.11
Cluster-Chr10-1	*qBNP-Chr10-1*	2016	bin1048	bin1049							3.24	0.94	6.40
	qLY-Chr10-1	2016	bin1048	bin1049							2.18	1.40	4.22
Cluster-Chr10-2	*qBW-Chr10-1*	2017	bin1074	bin1075	2.30	0.11	4.10						
	qPPF-Chr10-1	2016	bin1084	bin1085							2.97	4.48	5.97
Cluster-Chr11-1	*qLY-Chr11-1**	2018	bin1153	bin1154	2.11	1.33	4.10						
		2016	bin1153	bin1154				4.06	2.01	8.17			
	qPPF-Chr11-1	2018	bin1153	bin1154				3.04	3.92	5.85			
	qSY-Chr11-1	2018	bin1154	bin1155				2.53	3.06	4.86			
	*qLP-Chr11-1**	2017	bin1162	bin1163				2.25	−0.53	3.02			
		2016	bin1165	bin1166				2.35	−0.52	3.64			
Cluster-Chr12-1	*qSY-Chr12-1*	2016	bin1287	bin1287							2.32	3.39	4.61
	qPPF-Chr12-1	2016	bin1287	bin1288							2.73	4.22	5.49
	qBNP-Chr12-1	2016	bin1297	bin1298				2.32	0.70	4.76			
		2016	bin1297	bin1298							3.15	0.91	6.19
	qLP-Chr12-1	2017	bin1307	bin1308				2.08	−0.50	2.79			
Cluster-Chr13-1	*qBNP-Chr13-1*	2017	bin1441	bin1442				2.23	−0.75	4.41			
	qLP-Chr13-3	2016	bin1447	bin1448				2.97	0.60	4.63			
Cluster-Chr14-1	*qPPF-Chr14-1*	2016	bin1480	bin1481	3.78	4.79	7.20						
	qSY-Chr14-1	2016	bin1480	bin1481	3.09	3.71	5.90						
	*qBNP-Chr14-1**	2016	bin1479	bin1480	4.01	1.01	7.71						
		2017	bin1484	bin1485	2.27	0.72	4.36						
		2017	bin1484	bin1485				2.81	0.86	5.59			
	qSY-Chr14-2	2017	bin1484	bin1485				3.12	4.35	5.54			
	qBW-Chr14-1	2016	bin1492	bin1493				2.43	0.12	4.54			
Cluster-Chr14-2	*qPPF-Chr14-2*	2016	bin1508	bin1509							2.30	3.78	4.97
	qBNP-Chr14-2	2018	bin1508	bin1509							2.07	0.68	4.64
Cluster-Chr15-1	*qBNP-Chr15-1*	2018	bin1571	bin1572							2.57	0.74	5.51
	qPPF-Chr15-1	2017	bin1573	bin1574	2.34	4.18	4.54						
Cluster-Chr15-2	*qSY-Chr15-1*	2017	bin1605	bin1606				2.40	−3.67	3.98			
	*qBNP-Chr15-3**	2018	bin1605	bin1606				4.68	−0.85	9.63			
		2017	bin1609	bin1610				2.23	−0.75	4.40			
	qLP-Chr15-1	2017	bin1609	bin1610				2.10	−0.51	2.82			

(continued)

Table 5. (continued)

Cluster	QTL	Year	Flanking Marker		Under E1			Under E2			Mapping by the *D*-value		
			L	R	LOD	Effect value	Var%	LOD	Effect value	Var%	LOD	Effect value	Var %
Cluster-Chr16-1	*qLP-Chr16-1*	2017	bin1717	bin1718	4.73	−0.78	7.34						
	qLP-Chr16-2	2017	bin1723	bin1724	3.72	−0.69	5.85						
	*qPPF-Chr16-1**	2018	bin1721	bin1722				2.16	3.34	4.25			
		2016	bin1718	bin1719	3.66	−4.76	7.46						
	*qSY-Chr16-1**	2018	bin1719	bin1720				2.49	3.04	4.82			
		2016	bin1726	bin1727	2.82	−3.53	5.39						
		2018	bin1729	bin1730				2.78	3.25	5.36			
		2016	bin1731	bin1732							2.74	3.76	5.71
	*qPPF-Chr16-2**	2018	bin1730	bin1731				3.56	4.30	6.90			
		2016	bin1731	bin1732							3.26	4.72	6.83
		2016	bin1731	bin1732	4.73	−5.39	9.52						
	qBNP-Chr16-1	2018	bin1729	bin1730				2.49	0.59	5.03			
		2018	bin1734	bin1735				2.78	0.62	5.58			
	qBW-Chr16-1	2016	bin1731	bin1732	3.71	−0.14	6.74						
Cluster-Chr16-2	*qSY-Chr16-2**	2017	bin1796	bin1797							2.49	3.90	5.13
		2018	bin1797	bin1798	4.78	4.70	9.92						
	qPPF-Chr16-3	2018	bin1796	bin1797	4.40	5.98	9.25						
	qLY-Chr16-1	2017	bin1800	bin1801							2.95	1.87	5.96
	*qSY-Chr16-3**	2017	bin1807	bin1808							2.49	3.92	5.15
		2018	bin1809	bin1810	2.70	3.76	6.13						
Cluster-Chr18-1	*qLP-Chr18-1*	2016	bin1971	bin1972							2.19	−0.49	5.48
	qBNP-Chr18-1	2016	bin1967	bin1968	3.59	0.94	6.88						
Cluster-Chr19-1	*qLP-Chr19-1*	2018	bin2054	bin2055	2.39	−0.43	3.31						
	qLY-Chr19-1	2016	bin2056	bin2057	2.82	−1.52	5.51						
		2016	bin2065	bin2066	2.36	−1.38	4.64						
Cluster-Chr19-2	*qSY-Chr19-1*	2017	bin2101	bin2102	2.21	3.38	3.57						
	qLY-Chr19-2	2017	bin2101	bin2102	2.81	1.77	4.86						
	qLP-Chr19-2	2018	bin2112	bin2113							4.76	0.39	9.82
		2018	bin2113	bin2114				2.56	0.41	3.34			
Cluster-Chr20-1	*qBNP-Chr20-1*	2016	bin2229	bin2230	2.97	−0.85	5.63						
	qSY-Chr20-1	2017	bin2239	bin2240				2.65	−3.83	4.38			
	qPPF-Chr20-1	2017	bin2239	bin2240				2.14	−3.90	3.51			
Cluster-Chr21-1	*qLP-Chr21-1*	2017	bin2272	bin2273				2.86	0.62	4.10			
	qLY-Chr21-1	2016	bin2272	bin2273				4.10	1.71	8.40			
Cluster-Chr21-2	*qBNP-Chr21-1*	2017	bin2282	bin2283							2.72	0.96	5.23
	qPPF-Chr21-1	2016	bin2282	bin2283							3.56	6.16	7.26
Cluster-Chr21-3	*qBW-Chr21-1*	2016	bin2321	bin2322							2.09	0.13	4.41
	qBNP-Chr21-2	2017	bin2329	bin2330							3.52	−1.18	7.30
Cluster-Chr22-1	*qBW-Chr22-1*	2016	bin2463	bin2464	2.79	−0.12	5.30						
		2016	bin2470	bin2471	3.23	−0.13	5.63						
	qBNP-Chr22-1	2017	bin2470	bin2471							2.47	−0.89	4.45
	qLY-Chr22-1	2018	bin2471	bin2472	2.50	−1.47	4.97						
Cluster-Chr23-1	*qPPF-Chr23-1*	2016	bin2514	bin2515	2.02	3.62	4.26						
	qBW-Chr23-1	2016	bin2512	bin2513	2.30	0.11	3.97						
	qSY-Chr23-1	2017	bin2514	bin2515				3.84	4.81	6.95			
	qLY-Chr23-1	2018	bin2515	bin2516							2.06	1.13	4.22
Cluster-Chr23-2	*qSY-Chr23-2*	2016	bin2523	bin2524				3.86	3.91	7.74			
		2016	bin2533	bin2534	3.56	3.98	6.85						
	qPPF-Chr23-2	2016	bin2535	bin2536							2.47	5.29	4.97
		2016	bin2533	bin2534	4.51	5.23	8.68						
	qLY-Chr23-2	2016	bin2533	bin2534	4.15	1.88	8.25						
	qBNP-Chr23-1	2016	bin2535	bin2536	2.51	0.86	5.57						
Cluster-Chr24-1	*qLY-Chr24-1**	2018	bin2587	bin2588				2.28	1.70	4.99			
		2017	bin2587	bin2588				3.06	2.12	6.12			

(continued)

Table 5. (continued)

Cluster	QTL	Year	Flanking Marker		Under E1			Under E2			Mapping by the *D*-value		
			L	R	LOD	Effect value	Var%	LOD	Effect value	Var%	LOD	Effect value	Var %
		2017	bin2588	bin2589	2.83	1.86	5.38						
	qSY-Chr24-1	2017	bin2587	bin2588				3.05	4.30	5.55			
		2017	bin2588	bin2589	4.50	5.15	8.37						
	*qBW-Chr24-1**	2018	bin2593	bin2594				3.35	0.12	6.58			
	qPPF-Chr24-1	2017	bin2599	bin2600	2.17	4.09	4.22						
		2018	bin2599	bin2600				2.61	3.86	5.46			
		2017	bin2599	bin2600				6.44	7.56	12.71			
	qSY-Chr24-2*	2018	bin2600	bin2601				2.68	3.34	5.64			
		2017	bin2599	bin2600				3.93	5.03	7.08			
		2017	bin2599	bin2600	6.62	6.42	12.00						
	qBNP-Chr24-1	2017	bin2599	bin2600				3.81	1.00	7.68			
	qLY-Chr24-2*	2018	bin2599	bin2600				3.08	1.60	6.63			
		2017	bin2599	bin2600				5.04	2.75	9.81			
		2017	bin2599	bin2600	6.27	2.78	11.41						
	qBW-Chr24-1	2017	bin2604	bin2605	2.04	0.11	3.62						
Cluster-Chr24-2	*qBW-Chr24-2*	2016	bin2658	bin2659							3.28	−0.17	7.02
	qPPF-Chr24-2	2016	bin2659	bin2660							3.99	−6.79	8.21
Cluster-Chr25-1	*qSY-Chr25-1*	2018	bin2671	bin2672							2.01	2.61	4.34
	qLY-Chr25-1	2018	bin2677	bin2678							2.38	1.21	4.92
Cluster-Chr25-2	*qLP-Chr25-2*	2018	bin2722	bin2723				2.92	−0.47	4.35			
	*qPPF-Chr25-1**	2017	bin2727	bin2728	3.15	−4.82	6.18						
		2016	bin2729	bin2730				3.45	−4.27	6.79			
	qPPF-Chr25-2	2016	bin2744	bin2745				4.36	−4.67	8.48			
	qLY-Chr25-2*	2017	bin2737	bin2738	5.97	−2.62	10.67						
		2018	bin2741	bin2742				3.28	−1.52	6.33			
		2017	bin2742	bin2743				2.42	−1.82	4.56			
	*qLP-Chr25-3**	2017	bin2741	bin2742	4.31	−0.74	6.66						
		2018	bin2753	bin2754	2.66	−0.48	3.96						
		2017	bin2751	bin2752	3.20	−0.64	5.02						
	qBW-Chr25-1	2016	bin2755	bin2756	3.15	−0.13	5.82						
Cluster-Chr26-1	*qBW-Chr26-2*	2017	bin2833	bin2834				2.50	0.11	3.44			
	qSY-Chr26-1	2018	bin2833	bin2834	2.35	3.14	4.73						
	qLY-Chr26-1	2017	bin2840	bin2841				2.10	1.70	4.02			
		2017	bin2840	bin2841	2.67	1.74	4.75						
		2017	bin2844	bin2845	3.87	2.11	6.98						
		2017	bin2850	bin2851				3.01	2.01	5.69			
	qPPF-Chr26-1	2017	bin2844	bin2845	4.37	5.69	8.75						
	qBNP-Chr26-1	2017	bin2843	bin2844	3.82	0.91	7.78						
	qSY-Chr26-2	2017	bin2844	bin2845	3.97	4.71	6.96						
		2017	bin2853	bin2854				2.07	3.33	3.44			
	qPPF-Chr26-2	2017	bin2855	bin2856				2.54	4.36	4.43			

The figures underlined referred to the common QTL detected on two datasets in the same year in the present study. QTL with bold font represent the Var% of QTL was more than 10. QTL noted by "*" referred to common QTL detected at least 2 years; and Var%, phenotypic variation explained by a single locus QTL.
QTL, quantitative trait loci.

GhDAAT was a candidate gene in QTL *qBNP-Chr4-1* associated with salt tolerance

Salt stress affects the entire growth period of cotton. To identify salt related QTL in seeding stage and mature stage, we compared the salt related QTL with the QTL detected in germination and seedling stages under salt stress conditions (Guo, Hao, et al., 2022; Guo, Su, et al., 2022). The QTL (*qBNP-Chr4-1*) was overlapped with the interval of two QTL (*qMSH-Chr4-1* and *qSL-Chr4-1*) detected in the seedling stage, which controlled main stem height under salt stress conditions and controlled germinal length in *R*-value, respectively (Guo, Hao, et al., 2022; Guo, Su, et al., 2022). These two QTL (*qMSH-Chr4-1* and *qSL-Chr4-1*), explaining 7.50% and 9.59% of the PV, which were

detected in salt stress conditions and *R*-value, respectively. The confidence interval of *qBNP-Chr4-1* is between marker bin381 and bin385, corresponding to the reference genome of upland cotton TM-1 from 7 087 161 to 7 183 670 bp. The physical distance of this interval is 96 510 bp, including a single gene (*Gh_A04G0310*). The gene encoded a D-amino--acid transaminase (DAAT), may play an important role in salt stress response in upland cotton. To investigate the regulatory role of *GhDAAT* in salt tolerance, the tobacco rattle virus (TRV) system was used in the suppression of *GhDAAT* in upland cotton. The *GhCLA*-silenced plants showed a typical photobleaching phenotype in newly grown leaves, which indicated that the VIGS system was applied successfully in cotton (Figure 2a). We also examined the expression levels of *GhCLA* and *GhDAAT* in the gene-silenced plants by qRT-PCR. The gene expression was significantly decreased in gene-silenced plants (TRV:GhCLA and TRV:GhDAAT) than that in TRV:00 (plants transformed in empty vector) (Figure 2b,c). After 2 weeks treatment by 400 mM NaCl, TRV:GhDAAT plants showed a salt-sensitive phenotype, including a decreased seedling height and increased leave wilting rate when compared to the control plants (Figure 2d–g). Moreover, the malondialdehyde (MDA) content, POD, SOD, and CAT activities were detected in the leaves of TRV:GhDAAT and TRV:00 plants. Under the control condition, there was no significantly difference in MDA contents, SOD, POD and CAT activity between TRV:00 and TRV:GhDAAT plants. However, MDA contents was significantly increased, and antioxidant enzyme activity (SOD, POD and CAT activity) was significantly decreased in TRV:GhDAAT plants compared to TRV:00 (Figure 2h–k), suggesting that silencing of *GhDAAT* significantly suppressed salt tolerance in upland cotton.

Candidate genes covered by major QTL for LP

We focused on the stable QTL related to LP, which explained more than 10% of the observed PV across 3 years. The QTL (*qLP-Chr5-3*), explaining the PV from 13.30–32.74%, was detected in both salt stress conditions and normal growth conditions in 3 year trials. The confidence interval of *qLP-Chr5-3* is between marker bin633 and bin641, corresponding to the reference genome of upland cotton TM-1 83 534 339 to 85 222 043 bp. The physical

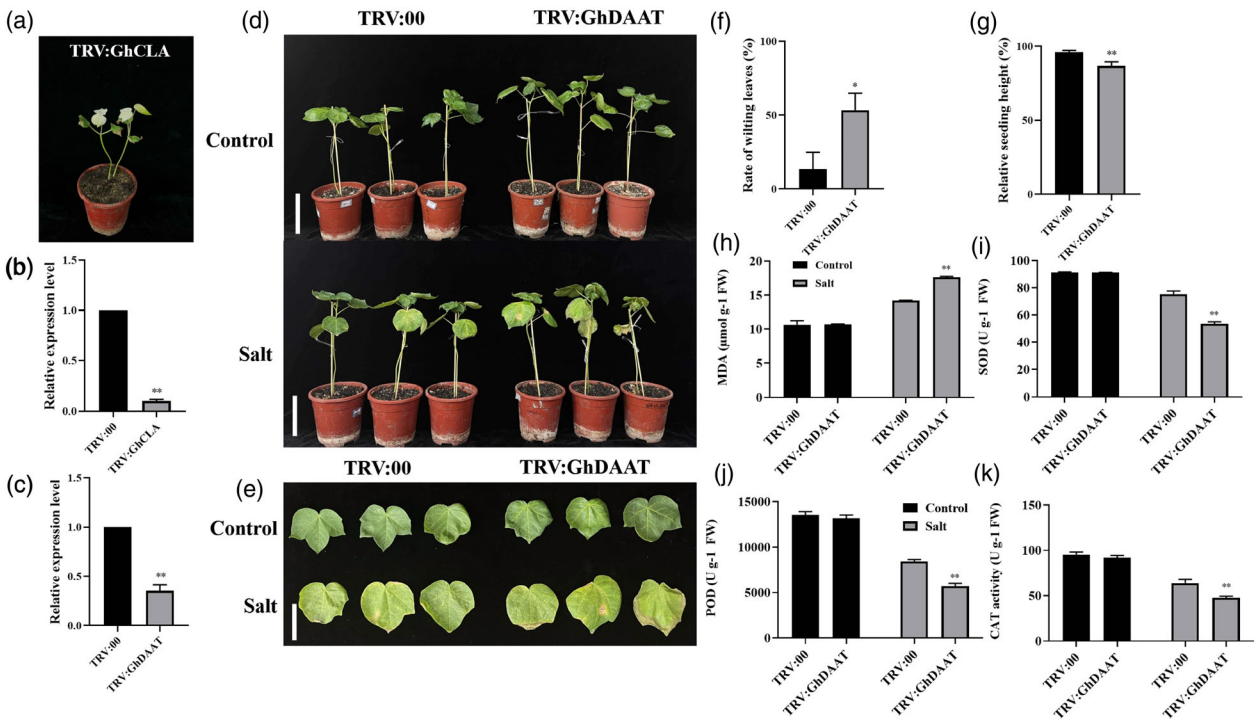

Figure 2. Silencing of *GhDAAT* decreased salt tolerance in upland cotton.
Phenotype identification (a) and silencing efficiency (b) of *GhCLA* in *GhCLA*-silenced plants.
(c) Silencing efficiency of *GhDAAT* in *GhDAAT*-silenced plants.
(d) Phenotypes of GhCDPKsk5-silenced plants after salt stress for 2 weeks (Scale bar = 10 cm).
(e) Phenotypes of leaves in GhCDPKsk5-silenced plants after salt stress treatment for 2 weeks (Scale bar = 5 cm).
The rate of wilting leaves (f) and relative seedling height (g) after salt stress treatment.
Malondialdehyde (MDA) contents (h) SOD (i), POD (j), CAT activities (k) in *GhDAAT*-silenced plants under control and salt stress treatments. Plants inoculated with 400 mM NaCl and deionized water for 2 weeks were used as salt stress conditions and control conditions, respectively. Except where noted, all data are presented as mean ($n \geq 3$) and standard deviation. Data were analyzed by Student's *t*-test. * and ** indicate significant differences between TRV:GhDAAT plants and TRV:00 plants at the $P = 0.05$ and $P = 0.01$ levels, respectively.

The Plant Journal published by Society for Experimental Biology and John Wiley & Sons Ltd.,
The Plant Journal, (2024), doi: 10.1111/tpj.16747

distance of this interval is 1 687 704 bp, including 77 genes (*Gh_A05G3184*–*Gh_A05G3260*) (Table S6).

Based on the 452 upland cotton RNA-seq data obtained from the National Genomics Data Center, the gene expressions during fiber development at the 19-time points (0, 3, 5, 7, 8, 10, 12, 13, 15, 16, 18, 19, 20, 21, 24, 25, 28, 30 DPA) were used for screening candidate genes involved in fiber development. We used a fold change of 2 as the threshold for identifying upregulated expression in comparisons between different time points and 0 DPA (Table S7). Genes with highly expression levels in 3 DPA, 4–20 DPA, and 21–30 DPA were screened as candidate genes which were involved in fiber initiation, fiber elongation, and SCW synthesis stage, respectively. A total of 32 candidate genes within *qLP-Chr5-3* showed high expression in the fiber initiation stage, and the fold change value for 15 genes was more than 5 (Figure S2a,b; Tables S7 and S8).

The QTL (*qLP-Chr5-3*) showed pleiotropy, which controlled fiber quality traits such as the fiber length (FL) and fiber strength (FS). To identify genes that regulate FL and FS within this QTL, we also analyzed genes that are highly expressed during fiber elongation and SCW thickening stages. In addition, 6 and 4 genes were highly expressed in fiber elongation stage (4–20 DPA) and SCW synthesis stage (21–30 DPA), respectively (Figure S3a,b; Tables S7 and S8).

To screen the candidate genes involved in fiber initiation at the transcriptional level, RNA-seq was performed on −1, 0, 3 DPA fibers obtained from high LP lines (RIL064 and RIL145), low LP lines (RIL131 and RIL093), and the parents (GX1135 and GX100-2). High-throughput RNA-Seq generated 560.07 Gb raw data from 54 RNA samples using the Illumina Novaseq Xplus platform, which was approximately 10.37 Gb for each sample. Overall, 93.00% (79.20–96.90%) of the high-quality reads were mapped to the TM-1 (*G. hirsutum*) reference genome. The average Q20, Q30, and GC contents were 98.88% (98.04–99.14%), 97.04% (95.40–97.59%), and 43.28% (40.76–44.51%), respectively (Table S9). The expression level of genes was calculated by transcripts per million reads (TPM) value after deleting the outlier (H1-1-2). In the comparison with the TM-1 reference genome, 49 279 genes were identified. In summary, the RNA-Seq provided abundant information, which facilitated exploring reliable transcription.

We analyzed the expression patterns of candidate genes in C high LP lines (GX1135, RIL064 and RIL145) and extremely low LP lines (GX100-2, RIL131 and RIL093) on −1, 0, 3 DPA. Most genes exhibited high expression levels in the fibers or ovules at −1, 0, 3 DPA except for one gene (*Gh_A05G3254*). The expression levels of all 11 genes in the low LP lines (GX100-2, L1, L2) were significantly higher than those in high LP lines (GX1135, H1, H2) (Figure S4). Furthermore, the expression patterns of candidate genes in two extremely high LP lines (RIL064, RIL145), two extremely low LP lines, and the parents (GX1135 and GX100-2) at the fiber initiation stage of fiber development were detected using qPCR. While the expression patterns of these genes varied, a notable commonality was observed: they exhibited higher expression levels in GX100-2 compared to GX1135, except for *Gh_A05G3254* (Figure 3). The expression levels in the extremely high LP lines (RIL064, RIL145) were higher than that of extremely

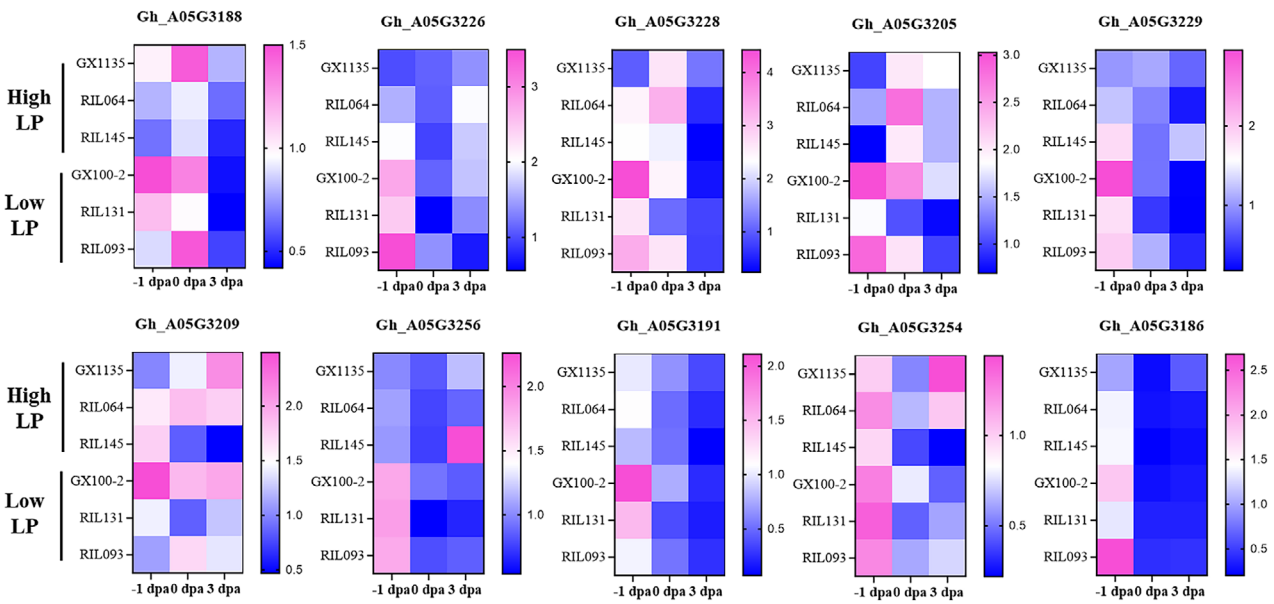

Figure 3. Expression patterns of candidate genes in GX1135, GX100-2 and extremely high/low LP lines during fiber initiation stages.
Two extremely high LP lines of RILs (RIL064 and RIL145) and the female GX1135 (high LP), two extremely low LP lines (RIL093, RIL131) and the male GX100-2 (low LP) were used for detect the expression levels at the fiber initiation stage. LP, lint percentage.

low LP lines (RIL093, RIL131) in at −1 DPA, which was consistent with the expression levels of the corresponding parents (Figure 3). The result suggests that these genes play important roles in fiber initiation.

Gene silencing of *qLP-Chr5-3* caused high LP and short FL

To further investigate the role of candidate genes within *qLP-Chr5-3*, we generated gene-silenced plants of 12 genes and evaluated yield and yield-component traits, fiber quality traits, and agronomic traits (plant height and branch number). The phenotype of *GhChlI*-silencing plants was visible in leaves, calyxes, and on surfaces of cotton bolls (Figure S7a–f). This indicated that the silencing phenotype induced by the cotton leaf crumple virus (CLCrV) system persisted, causing sustained photobleaching throughout the growth period of cotton. Of these genes, three genes encoding TF GTE4 were highly conserved (>90%). We designed special primers in the highly conserved region to ensure the silencing of all three genes. Finally, we constructed 10 VIGS vectors for 12 genes. qRT-PCR analysis indicated that the transcript levels of candidate genes in gene-silenced plants were decreased significantly than that in mock (Figure S8). In the field trials, silencing of four genes (*Gh_A05G3226*, *Gh_A05G3228*, *Gh_A05G3229*, *Gh_A05G3205*) significantly increased LP of 3.33–5.25% compared with mock (34.39%), and decreased FLM (manually measured FL) of 3.93–4.74% (Figure 4a–c; Table 6). Silenced genes highly expressed in fiber elongation stage resulted in 4.06–4.17% increases in LP and 2.41–3.59% decreases in FL (Figure 4a–c; Table 6). For genes highly expressed in the SCW stage, LP of plants silenced candidate genes was significantly increased from 2.09% to 6.03%, and FL was significantly reduced by 2.68–3.52% than that of mock (Figure 4a–c; Table 6). These results indicate that silencing highly expressed genes in fiber development stages increased LP and decreased FL. Moreover, two genes (*Gh_A05G3226* and *Gh_A05G3256*), encoding GTP-binding protein TypA/BipA and Glucan endo-1,3-beta-glucosidase 5, which controlled multiple yield-related traits. Specifically, silencing of *Gh_A05G3226* resulted in higher BW and lower BNP, while silencing of *Gh_A05G3256* increased LP, LY, BNP, and BW by 4.17%, 30.00%, 28.07%, and 10.32%, respectively (Figure 4; Table 6).

To identify the genetic elements of candidate genes contributing to the FL and LP traits, we explored the difference in candidate genes between the female and the male. No differences were observed in the coding sequence of *Gh_A05G3226* between GX1135 and GX100-2 (Figure S9). However, two nonsynonymous SNPs were detected in

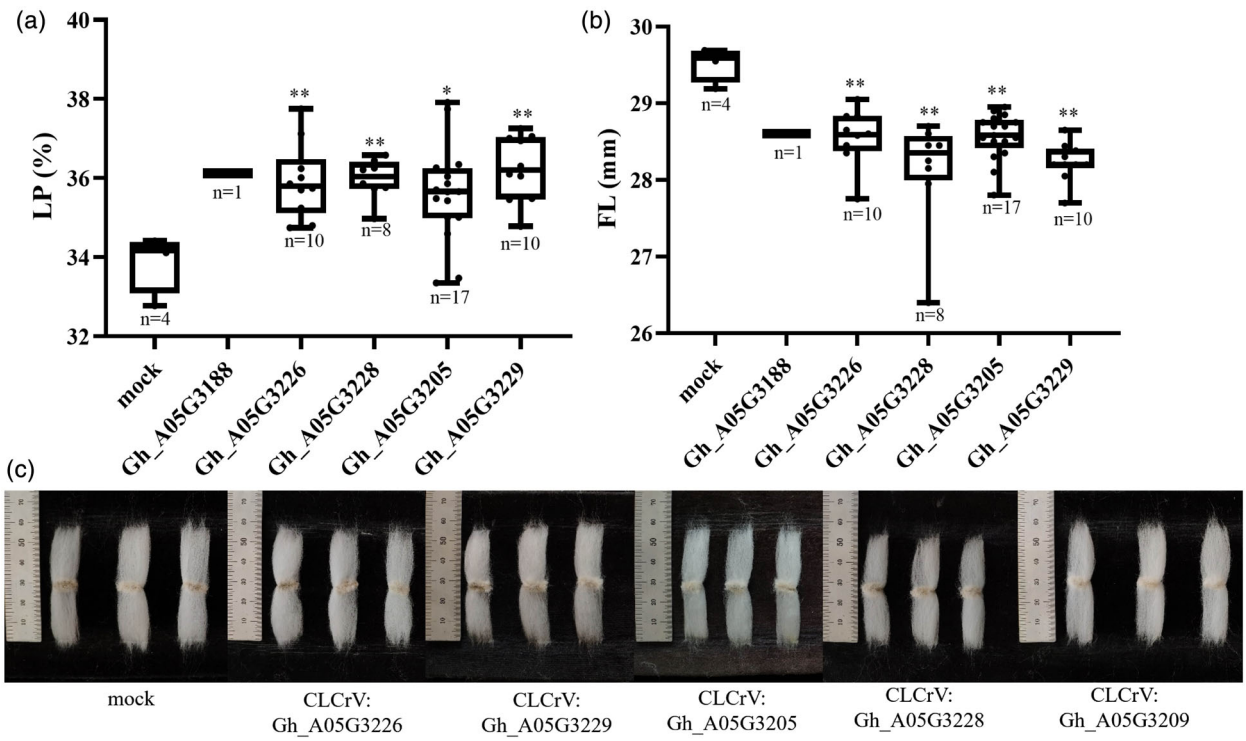

Figure 4. Silencing of candidate genes increased LP and decreased FL in upland cotton.
LP (a) and FL (b) of cotton plants silencing genes are highly expressed in the fiber development stage.
(c) The phenotype of mature fibers of gene-silenced cotton plants. FL, fiber length; LP, lint percentage. *, ** represent significant difference at $p = 0.05$, and $p = 0.01$ level, respectively.

Table 6 The agronomic traits, yield and yield-component traits, and fiber quality traits of genes-silenced plants

Gene	*N*	PH (cm)	BN	SY (g)	LY (g)	BNP	BW (g)	LP (%)	FLM
Gh_A05G3188	1	99.00	11.00	52.16	18.91	11.50	6.01	36.23	28.60
Gh_A05G3226	13	89.08	10.92	60.34	21.75	13.00*	5.69*	36.08**	28.36**
Gh_A05G3228	16	85.49	10.31	52.16	18.71	11.81	5.55	35.79**	28.12**
Gh_A05G3205	25	87.65	11.48	59.32	21.16	15.28	5.52	35.54**	28.57**
Gh_A05G3229	21	85.07	11.00	65.61	23.77	14.67	5.61	36.20**	28.23**
Gh_A05G3209	11	89.69*	11.45	62.07	22.24	17.27	5.51	35.79**	28.81**
Gh_A05G3256	14	82.09	11.43	73.64	26.35*	22.86*	5.56*	35.83**	28.46**
Gh_A05G3191	7	80.69	11.57	68.09	24.47	15.50	5.65	35.74*	28.73*
Gh_A05G3254	17	94.45**	11.94	65.83	24.05	14.76	5.60	36.47**	28.66**
Gh_A05G3186	14	87.76	11.64	67.10	23.57	19.71	5.24	35.11	28.48**
Mock	13	83.82	11.08	58.88	20.27	17.85	5.04	34.39	29.52

BN, branch number; BNP, boll number per plant; BW, boll weight; FLM, manually measured FL; LP, lint percentage; LY, lint yield per plant; PH, plant height; SY, seed cotton yield per plant.
*, ** Statistically significant at $P = 0.05$, 0.01, respectively.

Gh_A05G3186, which encodes WRKY 3. Two transversions were detected in the second exon, which includes a T/G transversion at the site of 802 and an A/G transversion at the site of 1106 (Figure S10a–c). Then we explored the genetic variants of *Gh_A05G3186* on the genome level using a population consisted of 349 upland cotton accessions. The phenotypically associated SNP (802) and SNP (1106) resulted in a T/G and A/G transversion, respectively, leading to tyrosine (Y)/aspartate (D), lysine (K)/arginine (R) (Figure S10a), which was associated with either shorter or longer fiber, respectively. Among 349 *G. hirsutum* accessions, 231 exhibited short/low strength fiber (TA), and 46 accessions had the long/high-strength fiber haplotype combination (TT) (Figure S10d,e) (unpublished data). However, there is no significant difference in LP between these two haplotypes (Figure S10f).

DISCUSSION

Effects of salt stress on yield-related traits in cotton

The cotton yield is seriously reduced when the total content of water-soluble salt in saline-alkali soil exceeds 2 g kg^{-1} (Table 1). For instance, the SY decreased by an average of 10.98% from 2017 to 2018. And the average decreased rate in 3 years' trial of BNP (15.44%) was the highest compared to the other yield related traits (SY: 13.52%; LY: 14.02%; BW: 0.41%; LP: 0.70%). In the present research, the total soluble salt content of saline soil in 2017 and 2018 were 2.79 and 2.03 g kg^{-1}, respectively, indicating moderate saline soil. And the soluble salt content of normal soil is 1.15 and 1.26 g kg^{-1} in 2017 and 2018, respectively, classifying it as mild saline-alkali soil (Tables S10 and S11) (Guo et al., 2021). Therefore, mild saline-alkali soil promotes the growth of cotton, while moderate saline-alkali soil reduces the yield of cotton. The yield reduction caused by salt stress was associated with the decrease of boll number per plant (BNP), but not boll weight (BW) and LP (Tables 1 and 3), which was consisted with the results of previous research (Zhu et al., 2020). The possible reason is salt stress inhibits plant photosynthesis and thus affects vegetative growth. It has been found that cotton yield can decrease by up to 90% when irrigated with saline water during the budding stage (Saidi & Hegazy, 1980). Salinity causes a decrease in the bolls number due to both decreased fruiting positions and an increase in the percentage of bolls shedding (Longenecker, 1973). The decline in mature bolls leads to a reduction in fruit-bearing position, delayed flowering, and relatively increased shedding of flowers and bolls under salt-stress conditions (Anagholi et al., 2013).

There were 44 and 43 QTL detected in the *D*-value and SI datasets for yield and yield component traits, respectively, of which 25 QTL were detected in both datasets, accounting for nearly 60%. The phenotypic variation of QTL interpretation detected in both datasets was consistent, indicating that the *D*-value dataset we established is reliable for the detection of salt-related QTL (Table S5). Among the salt-related QTL detected in these two datasets, BNP had the highest number of QTL for BNP, with 13 and 12 QTL in the *D*-value and SI datasets, respectively. Additionally, among the 25 QTL simultaneously detected in the *D*-value and SI datasets, those controlling BNP were the most numerous (nine). Overall, these salt-related QTL controlling BNP can be utilized to identify genes responding to salt stress in upland cotton.

QTL clusters control LP and FL/FS

Generally, LP is negatively correlated with FL and FS (Sun et al., 2018; Zhang et al., 2020). Hence, enhancing LP without compromising fiber quality traits (FL or FS) is challenging. The female GX1135 (39.03–44.21%) is superior to the

male GX100-2 (35.88–37.70%) for LP in most environments, except for the performance under E1 in 2017 (GX1135: 43.74%, GX100-2: 44.09%), while showed no significant difference for FL and FS (Guo et al., 2021). We obtained a consistent result using the phenotypic values of fiber quality traits and five yield-related traits collected in 19 environments in mutiple years (2012, 2015, 2016 and 2017) (Figure S5). The present RIL population makes it possible to improve LP and FL/FS simultaneously. However, the key genes were not identified, possibly due to limitations in linkage map density and the availability of high-quality genome information.

Quantitative trait loci for different traits (including fiber quality and yield) that shared the same confidence intervals were considered as QTL clusters, which indicated that the interval might harbor linked or pleiotropic genes that contributed to different traits (Abdelraheem et al., 2017). Five fiber quality traits (Guo et al., 2021) and five yield and yield component traits were used for QTL cluster identification. A total of 41 QTL clusters controlled both fiber quality and yield traits were detected, of which 21 and 20 were located on At and Dt sub-genome, respectively (Table S12). All these QTL clusters were distributed on 24 chromosomes except for Chr 3, Chr 10, Chr 12, and Chr 17. Among them, six QTL clusters controlling FS or FL and LP simultaneously, comprising three for FL and LP; two for FS and LP; and three for all three traits (FL, FS, and LP), respectively. The female GX1135 allele increased LP but decreased FL or FS in three clusters (Cluster-Chr5-1′, Cluster-Chr5-3′, Cluster-Chr13-1′) and it decreased LP but increased FL or FS in four clusters (Cluster-Chr11-1′, Cluster-Chr15-1′, Cluster-Chr15-2′ and Cluster-Chr25-3′). However, an interesting phenomenon was observed in the two clusters, showing that the additive effects of QTL for LP and FL were not always opposite. In Cluster-Chr1-2′, the favorable allele of *qFL-Chr1-1* was derived from the GX1135 in 2016, and GX100-2 in 2018, the favorable allele of *qLP-Chr1-2* was derived from the GX1135. Another cluster named Cluster-Chr25-2 harbored five QTL (*qSY-Chr25-2*, *qFE-Chr25-1*, *qFM-Chr25-1*, *qFS-Chr25-1* and *qLP-Chr25-1*), which decreased both FS and LP simultaneously. These clusters could be potential targets for molecular marker-assisted selection and map-based cloning for the improvement of LP and FL/FS (Zhang et al., 2019).

The most clusters (three) were identified on Chr 5, among which Cluster-Chr5-3′ controlled QTL for seven traits (yield: SY, LY, BW, LP; fiber: FL, FS, FM). This indicates the presence of numerous potential loci for yield and fiber quality improvement was on Chr 5.

Stable QTL for LP on Chr 5

Quantitative trait loci mapping was carried out using the phenotype data of five yield and yield component traits in 19 environments (Table S13) and compared with the QTL detected in the present study (Ma, Wang, Ijaz, & Hua, 2019; Ma, Wang, Li, et al., 2019; Shang et al., 2016). In present study, 151 QTL for five yield and yield component traits were detected in three datasets (E1, E2, and *D*-value), of which 42 QTL were detected in at least three environments. Among these, 11, 7, 6, 5, and 13 QTL for SY, LY, BNP, BW, and LP were detected, respectively. Four QTL were identified in at least 10 environments, including two QTL (*qBW-Chr5-1*, *qLP-Chr5-2*) detected in 19 environments, *qLP-Chr13-1* in 14 environments, and *qLP-Chr5-3* in 10 environments. Remarkably, three of these stable QTL (*qBW-Chr5-1*, *qLP-Chr5-2*, and *qLP-Chr5-3*) were detected on Chr5. The identification of the most stable QTL for LP aligns with the trait's highest heritability.

The QTL identified on the Chr5 were compared with those from the cotton QTL database, CottonGen database, and the previous researches using QTL mapping and genome-wide association studies (GWAS) based on the physical confidence intervals. Among the reported QTLs for LP, a total of 24 were identified. Notably, two of these QTLs, namely *qGhLP-c5* and *qLP-Chr05-1*, shared overlapping confidence intervals with *qLP-Chr5-1* and *qLP-Chr5-2* from the present study, respectively (Table S14) (Huang et al., 2017; Li et al., 2016). We also compared the published GWAS results with the physical location of the QTL for LP in Chr 5 and found that three QTL were consistent with the reported SNP associated with LP. Specifically, the intervals of qLP-At05, TM13226, and TM13292 were found to be consistent with *qLP-Chr5-1*, *qLP-Chr5-2*, and *qLP-Chr5-3*, respectively (Table S15) (Song et al., 2019; Zhu et al., 2020). It's worth noting that *qLP-Chr5-4* was a newly identified QTL on Chr 5 in the present research.

Multiple minor-effect genes clustered on the Chr 5 affect yield and fiber quality

The distribution of QTL on 26 chromosomes was uneven, indicating that different chromosomes contributed differently to LP. This can be explained by parental genetic diversity in different experiments. A RIL population derived from an upland cotton intraspecific cross between Nongdamian13 (high fiber quality) and Nongda601 (high yield) was used for QTL mapping for fiber quality and yield traits. The greatest number of QTL for LP was identified on Chr D02 (Gu et al., 2020). Moreover, most of the stable QTL controlled LP were detected on Chr 4, 6, 7, 13, 21, and 25, which was conducted by a RIL population derived from two upland cotton cultivars, 0–153 and sGK9708 (Zhang et al., 2020). An important cluster with LP and fiber quality traits (FL, FS, and FM) was detected in Chr D03 (Diouf et al., 2018). However, four QTL for LP (*qLP-Chr5-1*, *qLP-Chr5-2*, *qLP-Chr5-3*, *qLP-Chr5-4*) explained PV of 7.66–32.74% were detected in the present study, of which *qLP-Chr5-3* and *qLP-Chr5-4* were detected across 3 and 2 years, respectively.

In addition, the interval of *qLP-Chr5-2* showed a pleiotropic effect, which overlapped with the interval of the salt-tolerance QTL *qFER-Chr5-4*, and another QTL *qLP-Chr5-3* overlapped with the interval of five salt-tolerance QTL (*qFER-Chr5-4*, *qFW-Chr5-1*, *qDW-Chr5-1*, *qSH-Chr5-3*, and *qNL-Chr5-3*) (Figure S6). The results suggest that Chr 5 (A05) contributes to LP, FL, FS, and salt tolerance, which could be used for the improvement of cotton yield, fiber quality, and salt tolerance breeding. To screen genes associated with LP, FL, and FS, the expression patterns of genes within *qLP-Chr5-3* located on Chr 5 were identified based on the transcriptome analysis on different fiber development stages. In the interval of the QTL *qLP-Chr5-3*, 32, 6, and 4 genes were highly expressed in fiber initiation stage (−3 DPA to 3 DPA), fiber elongation stage (4–20 DPA), and SCW synthesis stage (21–30 DPA), respectively (Figures S2 and S3; Table S8). These genes were noted as candidates for LP, FL, and FS, respectively. Furthermore, the genes have high expressions in fiber initiation stage and function as negative regulators for LP. Silencing the candidate genes highly expressed in fiber development stages within *qLP-Chr5-3* resulted in an increase in LP and a decrease in FL (Table 4; Figure 4). It is suggested that the genes within *qLP-Chr5-3* act as minor effect genes clustered on Chr5, contributing to the control of fiber development in cotton.

Candidate genes involved in fiber cell differentiation and elongation

Peroxidase regulates many physiological processes, including the polymerization of cell wall compounds. The peroxidase coding gene *GhPOX1* was highly expressed in growing fiber cells, which may regulate fiber cell development by mediating reactive oxygen species production (Mei et al., 2009). In the present study, the gene (*Gh_A05G3239*) encoded peroxidase 43 was highly expressed in the fiber initiation stage (Figure S2b; Table S8).

Transcription factors have been shown to play an important role in fiber initiation and elongation, such as MYB, ERF, and bHLH families. The number of initial fiber cells in the 0 DPA ovules of *GhMYB5_A12* over-expressed cotton was increased significantly than that in wild-type plants, which indicated a positive role in fiber initiation (Wang, Jia, et al., 2021; Wang, Li, et al., 2021; Wang, Ma, et al., 2021). Overexpressed the *bHLH* gene (*GhFP2*) in cotton suppressed fiber elongation, while suppression of *GhFP2* expression led to longer fiber. And another *bHLH* gene, *GhACS*, acts as a positive role in regulating fiber elongation (Lu et al., 2022). A total of 52 ERFs were differentially expressed between 0 versus 5 DPA in upland cotton variety ZM24 (Zou et al., 2022). In the present study, three TFs (*GhGTEs*) were highly expressed during fiber initiation stage, which may act as positive roles in fiber initiation (Figure S2b; Table S8).

The GTPase (*GhRac1*) regulates fiber elongation by controlling cytoskeletal assembly (Kim & Triplett, 2004). Another gene, *Rac13*, has maximal expression at the time transition from primary wall synthesis to secondary wall synthesis, which plays an important role in the cytoskeletal organization (Delmer et al., 1995). In the present study, silenced the gene (*Gh_A05G3226*), which encodes GTP-binding protein TypA/BipA, increased LP from 34.39 to 36.08 in upland cotton (Table 6). The result indicated that the gene may involve in fiber development by regulating cytoskeleton formation. β-glucosidase (*BG*), which is one of the cellulases, was involved in the metabolism of cell wall polysaccharides (Zhu et al., 2011). It functions in the hydrolysis of cellobiose to glucose, which is involved in the degradation of cellulose–xyloglucan microfibrils and modification of newly deposited glucans during the developing cell wall process (Ma et al., 2006). *GhBG* was specifically expressed in the process of fiber development, which may affect cotton fiber SCW synthesis (Ma et al., 2006). The gene (*Gh_A05G3256*), encodes glucan endo-1,3-beta-glucosidase 5, was significantly upregulated in the fiber elongation stage (5–20 DPA) (Tables S6 and S8). Furthermore, silencing this gene resulted in higher yield (LP, LY, BNP, and BW) and shorter FL (Table 6). Although we have identified the genes that involved in fiber development and yield building, the molecular mechanism for fiber development is still not well enunciated. We still need to combine fine mapping to further verify the key genes and dissect the molecular mechanism of these genes involved in fiber development.

EXPERIMENTAL PROCEDURES

Plant materials

A RIL population derived from two upland cotton cultivars, GX1135 and GX100-2, was used in present study. The RIL population, which includes 177 lines of F_{15}–F_{17} generations, was used in the field evaluation from 2016 to 2018. The control set was performed in two field trials, including GX1135, "Xinza 1" F_1, GX100-2, and a commercial hybrid "Ruiza 816" used as a competitive control (Guo et al., 2021).

A total of 349 upland cotton accessions, comprising cultivars collected from different regions of China, were used for genotyping and population characteristic analysis.

For the VIGS experiment, *G. hirsutum* cultivar GX100-2 was used for salt tolerance assay in the greenhouse and for LP genes validation.

Field arrangement

Two field trials under salt stress conditions and normal growth conditions were conducted at the Quzhou Experimental Station of China Agricultural University, Handan City, Hebei Province (36°78′ N, 114°92′ E). Two independent field trials were arranged in neighboring fields following a randomized complete block design with two replications each in 2016, 2017, and 2018, respectively. A total of 362 plots with two rows (22 individual plants per row) were conducted, respectively. Two repeats of 177 RI Lines (F_{15}–F_{17}) were planted together with two control sets (GX1135, F_1

"Xinza 1", GX100-2, "Ruiza 816"). Field trials were described previously (Guo et al., 2021).

For salt stress treatment, shallow saline groundwater with a concentration of 5 g L^{-1} (85 mM) saline was used to irrigate the field in January and March before sowing. For the control treatment, regular irrigation with non-saline water was performed needed. Field management followed the local standard field practices.

The natural population of 349 accessions was planted in an experimental field across 3 years (2017–2019) with a randomized complete block design with two replications. Four locations were comprised of Hejian City in Hebei Province, Shijiazhuang City in Hebei Province, Yuncheng City in Shanxi Province, and Korla City in Xinjiang Uyghur Autonomous Region.

Soil sample collection and component detection

Soil samples were collected from a depth of 20–40 cm. To cover the experiment area, we sampled the points every 15 m from north to south in the experiment field. Three soil samples collected for each sample site were mixed into one sample for testing soil salinity. Soil-saturated paste extracts (1:2 by weight) were prepared to measure the electrical conductivity and total content of water-soluble salt (ρ) (Rhoades, 1996).

Trait evaluation and dataset's constitution

A total of six yield and yield component traits of 177 RILs were used for QTL mapping, which included SY (gram per plant), LY (gram per plant), BNP, BW (g), and LP (%). Bolls from eight plants, including four consecutive plants starting from the second individual in the first row, and four plants in the second row of each block, were sampled under salt and normal conditions, respectively. Boll samples were ginned for SY, LY, BNP, BW, and LP (Shang et al., 2016). To reflect the effect of salt stress on cotton yield, the composite trait—PPF was established in present research: PPF (g) = BNP × BW.

Three datasets of salt stress conditions (E1), and normal growth conditions (E2), the *D*-value, and the SI dataset were used for QTL mapping. The original phenotype values of five yield and yield component traits were obtained from the trials under E1 and E2, respectively. The establishment of the *D*-value has been described as referring to our previous research (Guo et al., 2021). A constant ($C = 100$) was added to the difference values between salt stress and normal growth conditions to ensure the *D*-value was positive. The salt index = (phenotype value of trait under normal growth conditions − phenotype value of trait under salt stress conditions)/phenotype value of trait under normal growth conditions × 100. A constant ($C = 500$) was added to the SI values to transfer the SI as positive value.

Five yield and yield component traits and two agronomic traits (plant height, PH, branch number, BN) of gene-silenced plants were evaluated. PH was recorded by measuring the main-stem height of cotton plants (Shang et al., 2015).

The phenotype analysis of 349 upland cotton accession, including the FL, FS, and LP, was conducted. The fiber quality evaluation was described as our previous research (Guo et al., 2021). Phenotyping of three traits was performed across four locations over 3 years.

Genetic linkage map and QTL mapping

The genetic map for the RIL population has been reported (Guo et al., 2021). The genetic linkage map consisting of 2859 bins, spanning 2133.53 cM of the total recombination length, was constructed with an average interval of 0.785 cM.

The experimental data were analyzed by the software SPSS (Version 20.0; SPSS, Chicago, IL, USA). Single-locus QTL was detected using the composite interval mapping (CIM) method by the software WinQTL Cartographer software 2.5 (Wang et al., 2007). We set parameters in the confidence interval of 95% with the CIM method for QTL mapping. The threshold of LOD value was estimated by 1000 permutations tests to declare a significant QTL with a significance level of $P < 0.05$, whereas the same QTL in two or three environments with LOD of at least 2.0 were considered as common QTL (Shang et al., 2016).

Candidate gene identification and annotation

Genes within the candidate QTL were fetched from the CottonGen (https://www.cottongen.org) using their flanking marker positions in the TM-1 (*G. hirsutum*) genome. To further screen the candidate genes involved in fiber development, the gene expression pattern of genes in different periods of fiber development was conducted using the 425 published RNA-seq data.

Candidate genes with high expression at fiber initiation stage were screened according to the following criteria: TPM value >1, and the fold change (TPM value in fiber initiation stage/fiber elongation stage) >5, are defined as genes with high expression at fiber initiation.

RNA extraction and RNA sequencing analysis

RNA was extracted from the mixture of ovules and fibers at −1, 0, 3 DPA for RNA sequencing (RNA-seq). The samples were poured into a mortar that was flash-frozen in liquid nitrogen. Total RNA was extracted using an RNAprep Pure Plant Kit (Polysaccharides & Polyphenolics-Rich) (Tiangen, Beijing, China) according to the manual provided by the manufacturer. A total of 1 μg RNA per sample was used for the RNA sample preparation and sequencing libraries construction. The library preparations were sequenced on the Illumina Novaseq Xplus platform using the PE150 model. FastQC was used for sequencing quality assessment and to obtain clean data. After screening and trimming, clean reads were mapped to cotton reference genome (*G. hirsutum* TM-1_V1.1, NBI) (Zhang et al., 2015) using STAR (Dobin et al., 2013). FeatureCounts was used to count the reads mapped to each gene (Love et al., 2014). Details of the genome mapping are provided in Table S9. Gene expression levels were estimated as TPM values. The differentially expressed genes between high LP lines (GX1135, RIL064, RIL145) and low LP lines (GX100-2, RIL093 RIL131) were performed using DESeq2 (Love et al., 2014) in R with a false discovery rate <0.05 and $|\log_2 \text{FoldChange}| > 1$.

Gene expression analysis by qRT-PCR

Total RNA was isolated from −1, 0, 3, 5, 10, 15, and 20 DPA fibers in female (GX1135) and male (GX100-2), respectively. To validate the potential function of candidate genes in fiber development, the expression patterns were verified using cDNA of different developmental fiber stages of GX11135 and GX100-2 by qRT-PCR. The relative expression level of candidate gens was calculated with the $2^{-\Delta\Delta Ct}$ method (Livak & Schmittgen, 2001). Primers for the qRT-PCR analysis are listed in Table S16. Three independent replicates were performed for each sample. *GhUBQ7* gene was used as a reference gene.

VIGS analysis in upland cotton

CLCrV and TRV systems were used for the validation of LP related genes and salt stress related genes, respectively. The CLCrV-fused cDNA fragment of *GhChlI* (magnesium chelatase subunit I) and

TRV-fused cDNA fragment of *GhCLA* (chloroplasts alterados 1) were used as a positive control to monitor the efficiency of VIGS experiments. The fragments targeting the candidate genes were integrated into CLCrVA or TRV2. All vectors constructed were transformed into *Agrobacterium tumefaciens* strain GV3101 by a heat-shock method. The GV3101 line contained CLCrVA (mock), and CLCrVA-genes vectors was mixed with an equal volume of *A. tumefaciens* containing CLCrVB, respectively. The GV3101 contained TRV:00, and TRV:GhDAAT vectors were mixed with an equal volume of *A. tumefaciens* containing TRV1. Then, the mixed solution was used to infiltrate plants. qRT-PCR was performed to further confirm that candidate genes had been silenced in VIGS experiments. The primers used in the qRT-PCR analysis and vector construction are listed in Table S16.

The cotyledons of 1-week-old cotton seedlings were used for infiltration according to the previous description (Guo, Hao, et al., 2022). The gene-silenced cotton plants for LP candidate genes were planted in the field in Hejian, Cangzhou City, Hebei Province (38°45′ N, 116°10′ E).

The gene-silenced cotton plants for *GhDAAT* were plants in the greenhouse for salt treatments. For salt tolerance treatment, cotton seedlings infiltrated with *A. tumefaciens* of TRV:00 and TRV:GhDAAT after 2 weeks were irrigated by 400 mM NaCl solution regularly every 4 days until the phenotype appeared (Guo, Hao, et al., 2022).

AUTHOR CONTRIBUTIONS

AG, HL, and XM performed all experiments, AG finished the data analysis and the manuscript preparation. YH, BL, XD, NZ, and YC attended bench work and discussion. JH conceived the experiments, provided the experimental platform, YH and JH revised the manuscript. All authors approved the final version of the manuscript.

ACKNOWLEDGMENTS

This research was supported by the National Natural Science Foundation of China (32201713 to A. G. and 32372128 to J. H.). We thank Dr. Lingling Ma and Dr. Ying Su for their contributions on data collection and primary analysis of trials in 2016 and 2017, respectively. We thank Prof. Pengbo Li (Institute of Cotton Research, Shanxi Agricultural University, Yuncheng, China), Prof. Baosheng Guo (Cotton Research Institute, Hebei Academy of Agriculture and Forestry Sciences, Shijiazhuang, China) and Prof. Jie Kong (Institute of Economic Crops, Xinjiang Academy of Agricultural Sciences, Ürümqi, China) for the collection of fiber quality traits and lint percentage trait of 349 upland cotton accessions. We thank Prof. Guanjing Hu and Dr. Xianpeng Xiong (Agricultural Genomics Institute at Shenzhen, Chinese Academy of Agricultural Sciences, Shenzhen, China) for providing the transcriptome data of candidate genes at fiber development stages.

CONFLICT OF INTEREST

The authors declare that there are no conflicts of interest.

DATA AVAILABILITY STATEMENT

All the supplementary material files are available in the supporting information. The high-density linkage map has been published at https://doi.org/10.1007/s00122-020-03721-x.

SUPPORTING INFORMATION

Additional Supporting Information may be found in the online version of this article.

Figure S1. The position of QTL for five yield and yield-component traits on the linkage groups.

Figure S2. Expression patterns of genes highly expressed in fiber initiation stage. The TPM value of genes was used for drawing heatmap. Data are retrieved from the public database. (a) Fold change >5; (b) Fold change >2.

Figure S3. Expression patterns of genes highly expressed in fiber elongation stage and fiber secondary cell wall synthesis stage. (a) Expression patterns of genes highly expressed in fiber elongation stage; (b) expression patterns of genes in secondary cell wall synthesis stage.

Figure S4. Expression patterns of candidate genes in extremely high LP lines low LP lines, and parents of RILs at fiber initiation stage. F, H1, H2 represent GX1135, RIL131, RIL093; M, L1, L2 represent GX100-2, RIL064, RIL145, respectively. −1, 0, 3, represent −1, 0, and 3 DPA, respectively. Expression levels = $\log_{10}(\text{TPM}+1)$.

Figure S5. The phenotype values of fiber quality traits and yield and yield-component traits of GX1135 and GX100-2 in 19 environments.

Figure S6. The position of QTL for LP, FL and salt tolerance traits on the Chr5.

Figure S7. Silencing of the *GhChlI* gene in upland cotton. The *GhChlI*-silenced cotton plant at seedling stage (a) and anthesis stage (b). Photobleaching phenotype observed in leaf (c), calyx (d) and boll (e) of *GhChlI*-silenced plants. (f) Relative expression level of *GhChlI* in leaves from *ChlI*-silenced or mock plants were detected by qRT-PCR. Data are presented as the mean ± standard error (SE) of three independent experiments in which three independent plants were included per experiment.

Figure S8. Gene silencing efficiency identification in gene-silenced plants. Relative expression level of candidate genes in fibers from gene-silenced or mock plants were detected by qRT-PCR. Data are presented as the mean ± standard error (SE) of three independent experiments in which three independent plants were included per experiment.

Figure S9. Nucleic acid sequence alignment of *Gh_A05G3226* in the female GX1135 and the male GX100-2.

Figure S10. Analysis of haplotypes in *Gh_A05G3186*. (a) Structure of *Gh_A05G3186*. Blue and yellow rectangles mark UTR and CDS respectively. Box plot for FL (b), FS (c), and LP (d) based on the haplotypes of the two SNPs. In the box plots, the center line indicates the median. Box limits are the upper and lower quartiles, and whiskers mark the range of the data; n denotes the number of accessions with the same genotype. We used a two-tailed *t*-test to perform the significance analysis. Single (*) and double (**) asterisks mark statistical significance levels of $P < 0.05$ and 0.01, respectively. (e, f) The SNPs in the CDS of *Gh_A05G3186* between GX1135 and GX100-2.

Table S1. Descriptive statistical analysis on the difference values dataset between salt stress and normal conditions for yield and yield-component traits.

Table S2. Descriptive statistical analysis on the salt index (SI) dataset for yield and yield-component traits.

Table S3. Correlation analysis among yield and yield-component traits under salt stress conditions, normal growth conditions, and *D*-value dataset.

Table S4. Single locus QTL for yield and yield-component traits under salt stress conditions, normal growth conditions and in *D*-value dataset.

Table S5. Single locus QTL for yield and yield-component traits in SI dataset.

Table S6. Annotation of genes within the QTL *qLP-chr5-3*.

Table S7. The TPM value of genes within the QTL qLP-chr5-3 in fiber development phrase.

Table S8. The description of genes within *qLP-Chr5-3* highly expressed in fiber initiation stage, fiber elongation stage and secondary wall thickening stage.

Table S9. Summary of generated read data, quality control and mapping on the TM-1 genome for all samples.

Table S10. The sample properties of salinity from EC and ρ.

Table S11. Grading standards for saline soil.

Table S12. Pleiotropic regions for fiber quality traits and yield and yield-component traits.

Table S13. QTL for yield and yield-component traits detected in 19 environments.

Table S14. The congruence analysis results with the previous QTL (same with QTLdatabase).

Table S15. The congruence analysis results with the previous QTL (same with GWAS).

Table S16. Primers used in VIGS experiments and qPCR analysis.

REFERENCES

Abdelraheem, A., **Feng, L.**, **Song, M.** & **Zhang, J.** (2017) A meta-analysis of quantitative trait loci for abiotic and biotic stress resistance in tetraploid cotton. *Molecular Genetics and Genomics*, **292**, 1–15.

Anagholi, A., **Esmaeili, S.**, **Soltani, V.** & **Khaffarian, H.** (2013) *Effects of salt stress on the growth and yield of cotton at different stages of development*. National Salinity Research Center. Food and Agriculture Organization of the United Nations.

Ashraf, J., **Zuo, D.**, **Wang, Q.**, **Malik, W.**, **Zhang, Y.**, **Abid, M.A.** ***et al.*** (2018) Recent insights into cotton functional genomics: progress and future perspectives. *Plant Biotechnology Journal*, **16**, 699–713.

Delmer, D.P., **Pear, J.R.**, **Andrawis, A.** & **Stalker, D.M.H.U.** (1995) Genes encoding small GTP binding proteins analogous to mammalian rac are preferentially expressed in developing cotton fibers. *Molecular & General Genetics*, **248**, 43–51.

Diouf, L., **Magwanga, R.**, **Gong, W.**, **He, S.**, **Pan, Z.**, **Jia, Y.** ***et al.*** (2018) QTL mapping of fiber quality and yield-related traits in an intra-specific upland cotton using genotype by sequencing (GBS). *International Journal of Molecular Sciences*, **19**, 441.

Diouf, L., **Pan, Z.**, **He, S.**, **Gong, W.**, **Jia, Y.**, **Magwanga, R.** ***et al.*** (2017) High-density linkage map construction and mapping of salt-tolerant QTLs at seedling stage in upland cotton using genotyping by sequencing (GBS). *International Journal of Molecular Sciences*, **18**, 2622.

Dobin, A., **Davis, C.A.**, **Schlesinger, F.**, **Drenkow, J.**, **Zaleski, C.**, **Jha, S.** ***et al.*** (2013) STAR: ultrafast universal RNA-seq aligner. *Bioinformatics*, **29**, 15–21.

Gu, Q., **Ke, H.**, **Liu, C.**, **Lv, X.**, **Sun, Z.**, **Liu, Z.** ***et al.*** (2021) A stable QTL *qSalt-A04-1* contributes to salt tolerance in the cotton seed germination stage. *Theoretical and Applied Genetics*, **134**, 2399–2410.

Gu, Q., **Ke, H.**, **Liu, Z.**, **Lv, X.**, **Sun, Z.**, **Zhang, M.** ***et al.*** (2020) A high-density genetic map and multiple environmental tests reveal novel quantitative trait loci and candidate genes for fibre quality and yield in cotton. *Theoretical and Applied Genetics*, **133**, 3395–3408.

Guo, A., **Hao, J.**, **Su, Y.**, **Li, B.**, **Zhao, N.**, **Zhu, M.** ***et al.*** (2022) Two aquaporin genes, *GhPIP2;7* and *GhTIP2;1*, positively regulate the tolerance of upland cotton to salt and osmotic stresses. *Frontiers in Plant Science*, **12**, 780486.

Guo, A., **Su, Y.**, **Huang, Y.**, **Wang, Y.**, **Nie, H.**, **Zhao, N.** ***et al.*** (2021) QTL controlling fiber quality traits under salt stress in upland cotton (*Gossypium hirsutum* L.). *Theoretical and Applied Genetics*, **134**, 661–685.

Guo, A., **Su, Y.**, **Nie, H.**, **Li, B.**, **Ma, X.** & **Hua, J.** (2022) Identification of candidate genes involved in salt stress response at germination and seedling stages by QTL mapping in upland cotton. *G3: Genes, Genomes, Genetics*, **12**, jkac099.

Huang, C., **Nie, X.**, **Shen, C.**, **You, C.**, **Li, W.**, **Zhao, W.** ***et al.*** (2017) Population structure and genetic basis of the agronomic traits of upland cotton in China revealed by a genome-wide association study using high-density SNPs. *Plant Biotechnology Journal*, **15**, 1374–1386.

Hussain, B., **Lucas, S.J.**, **Ozturk, L.** & **Budak, H.** (2017) Mapping QTLs conferring salt tolerance and micronutrient concentrations at seedling stage in wheat. *Scientific Reports*, **7**, 1–14.

Ismail, A.M. & **Horie, T.** (2017) Genomics, physiology, and molecular breeding approaches for improving salt tolerance. *Annual Review of Plant Biology*, **68**, 405–434.

Khorsandi, F. & **Anagholi, A.** (2009) Reproductive compensation of cotton after salt stress relief at different growth stages. *Journal of Agronomy and Crop Science*, **195**, 278–283.

Kim, H.J. & **Triplett, B.A.** (2004) Characterization of GhRac1 GTPase expressed in developing cotton (*Gossypium hirsutum* L.) fibers. *Biochimica et Biophysica Acta (BBA) - Gene Structure and Expression*, **1679**, 214–221.

Li, C., **Dong, Y.**, **Zhao, T.**, **Li, L.**, **Li, C.**, **Yu, E.** ***et al.*** (2016) Genome-wide SNP linkage mapping and QTL analysis for fiber quality and yield traits in the upland cotton recombinant inbred lines population. *Frontiers in Plant Science*, **7**, 1356.

Li, J., **Pu, L.**, **Han, M.**, **Zhu, M.**, **Zhang, R.** & **Xiang, Y.** (2014) Soil salinization research in China: advances and prospects. *Journal of Geographical Sciences*, **24**, 943–960.

Livak, K.J. & **Schmittgen, T.D.** (2001) Analysis of relative gene expression data using real-time quantitative PCR and the $2^{-\Delta\Delta CT}$ method. *Methods*, **25**, 402–408.

Longenecker, D.E. (1973) The influence of high Na^+ in salts upon fruiting and shedding boll characteristics, fiber properties and yield of two cotton species. *Soil Science*, **115**, 294–302.

Love, M.I., **Huber, W.** & **Anders, S.** (2014) Moderated estimation of fold change and dispersion for RNA-seq data with DESeq2. *Genome Biology*, **15**, 550.

Lu, R., **Li, Y.**, **Zhang, J.**, **Wang, Y.**, **Zhang, J.**, **Li, Y.** ***et al.*** (2022) The bHLH/HLH transcription factors GhFP2 and GhACE1 antagonistically regulate fiber elongation in cotton. *Plant Physiology*, **189**, 628–643.

Ma, G., **Zhang, T.** & **Guo, W.** (2006) Cloning and characterization of cotton *GhBG* gene encoding β-glucosidase. *DNA Sequence*, **17**, 355–362.

Ma, L., **Wang, Y.**, **Ijaz, B.** & **Hua, J.** (2019) Cumulative and different genetic effects contributed to yield heterosis using maternal and paternal backcross populations in upland cotton. *Scientific Reports*, **9**, 3984.

Ma, X., **Wang, Z.**, **Li, W.**, **Zhang, Y.**, **Zhou, X.**, **Liu, Y.** ***et al.*** (2019) Resequencing core accessions of a pedigree identifies derivation of genomic segments and key agronomic trait loci during cotton improvement. *Plant Biotechnology Journal*, **17**, 762–775.

Ma, Z., **Zhang, Y.**, **Wu, L.**, **Zhang, G.**, **Sun, Z.**, **Li, Z.** ***et al.*** (2021) High-quality genome assembly and resequencing of modern cotton cultivars provide resources for crop improvement. *Nature Genetics*, **53**, 1385–1391.

Mei, W., **Qin, Y.**, **Song, W.**, **Li, J.** & **Zhu, Y.** (2009) Cotton *GhPOX1* encoding plant class III peroxidase may be responsible for the high level of reactive oxygen species production that is related to cotton fiber elongation. *Journal of Genetics and Genomics*, **36**, 141–150.

Oluoch, G., **Zheng, J.**, **Wang, X.**, **Khan, M.K.R.**, **Zhou, Z.**, **Cai, X.** ***et al.*** (2016) QTL mapping for salt tolerance at seedling stage in the interspecific cross of *Gossypium tomentosum* with *Gossypium hirsutum*. *Euphytica*, **209**, 223–235.

Rhoades, J.D. (1996) Salinity: electrical conductivity and total dissolved solids. *Chemical Methods*, **142**, 417–435.

Saidi, M.E. & **Hegazy, W.** (1980) Effect of using saline water for irrigation at different growth stages on yield and some physiological processes of cotton plant. *Agricultural Research Review*, **58**, 337–355.

Shang, L., **Liang, Q.**, **Wang, Y.**, **Zhao, Y.**, **Wang, K.** & **Hua, J.** (2016) Epistasis together with partial dominance, over-dominance and QTL by environment interactions contribute to yield heterosis in upland cotton. *Theoretical and Applied Genetics*, **129**, 1429–1446.

Shang, L., **Liu, F.**, **Wang, Y.**, **Abduweli, A.**, **Cai, S.**, **Wang, K.** ***et al.*** (2015) Dynamic QTL mapping for plant height in upland cotton (*Gossypium hirsutum*). *Plant Breeding*, **134**, 703–712.

Song, C., **Li, W.**, **Pei, X.**, **Liu, Y.**, **Ren, Z.**, **He, K.** ***et al.*** (2019) Dissection of the genetic variation and candidate genes of lint percentage by a genome-wide association study in upland cotton. *Theoretical and Applied Genetics*, **132**, 1991–2002.

Sun, Z., **Wang, X.**, **Liu, Z.**, **Gu, Q.**, **Zhang, Y.**, **Li, Z.** ***et al.*** (2018) A genome-wide association study uncovers novel genomic regions and candidate genes of yield-related traits in upland cotton. *Theoretical and Applied Genetics*, **131**, 2413–2425.

Wang, H., **Jia, X.**, **Kang, M.**, **Li, W.**, **Fu, X.**, **Ma, L.** ***et al.*** (2021) QTL mapping and candidate gene identification of lint percentage based on a recombinant inbred line population of upland cotton. *Euphytica*, **217**, 102.

Wang, N., **Li, Y.**, **Chen, Y.**, **Lu, R.**, **Zhou, L.**, **Wang, Y.** ***et al.*** (2021) Phosphorylation of WRKY16 by MPK3-1 is essential for its transcriptional activity during fiber initiation and elongation in cotton (*Gossypium hirsutum*). *The Plant Cell*, **33**, 2736–2752.

Wang, N., **Ma, Q.**, **Wu, M.**, **Pei, W.**, **Song, J.**, **Jia, B.** ***et al.*** (2021) Genetic variation in MYB5_A12 is associated with fibre initiation and elongation in tetraploid cotton. *Plant Biotechnology Journal*, **19**, 1892–1894.

Wang, S., **Basten, C.J.** & **Zeng, Z.B.** (2007) *Windows QTL cartographer 2.5*. Raleigh, NC: Department of Statistics, North Carolina State University.

Zhang, K., **Kuraparthy, V.**, **Fang, H.**, **Zhu, L.**, **Sood, S.** & **Jones, D.C.** (2019) High-density linkage map construction and QTL analyses for fiber quality, yield and morphological traits using CottonSNP63K array in upland cotton (*Gossypium hirsutum* L.). *BMC Genomics*, **20**, 889.

Zhang, M., **Zheng, X.**, **Song, S.**, **Zeng, Q.**, **Hou, L.**, **Li, D.** ***et al.*** (2011) Spatio-temporal manipulation of auxin biosynthesis in cotton ovule epidermal cells enhances fiber yield and quality. *Nature Biotechnology*, **29**, 453–458.

Zhang, T., **Hu, Y.**, **Jiang, W.**, **Fang, L.**, **Guan, X.**, **Chen, J.** ***et al.*** (2015) Sequencing of allotetraploid cotton (*Gossypium hirsutum* L. acc. TM-1) provides a resource for fiber improvement. *Nature Biotechnology*, **33**, 531–537.

Zhang, Z., **Li, J.**, **Jamshed, M.**, **Shi, Y.**, **Liu, A.**, **Gong, J.** ***et al.*** (2020) Genome-wide quantitative trait loci reveal the genetic basis of cotton fibre quality and yield-related traits in a *Gossypium hirsutum* recombinant inbred line population. *Plant Biotechnology Journal*, **18**, 239–253.

Zhu, G., **Gao, W.**, **Song, X.**, **Sun, F.**, **Hou, S.**, **Liu, N.** ***et al.*** (2020) Genome-wide association reveals genetic variation of lint yield components under salty field conditions in cotton (*Gossypium hirsutum* L.). *BMC Plant Biology*, **20**, 23.

Zhu, H., **Han, X.**, **Lv, J.**, **Zhao, L.**, **Xu, X.**, **Zhang, T.** ***et al.*** (2011) Structure, expression differentiation and evolution of duplicated fiber developmental genes in *Gossypium barbadense* and *G. hirsutum*. *BMC Plant Biology*, **11**, 40.

Zhu, L., **Andres, R.J.**, **Zhang, K.** & **Kuraparthy, V.** (2021) High-density linkage map construction and QTL analysis of fiber quality and lint percentage in tetraploid cotton. *Crop Science*, **61**, 3340–3360.

Zou, X., **Ali, F.**, **Jin, S.**, **Li, F.** & **Wang, Z.** (2022) RNA-Seq with a novel glabrous-ZM24fl reveals some key lncRNAs and the associated targets in fiber initiation of cotton. *BMC Plant Biology*, **22**, 61.